Bioinspired control of colloidal silica *in vitro* by dual polymeric assemblies of zwitterionic phosphomethylated chitosan and polycations or polyanions

Konstantinos D. Demadis *, Konstantinos Pachis, Antonia Ketsetzi, Aggeliki Stathoulopoulou

Crystal Engineering, Growth and Design Laboratory, Department of Chemistry, University of Crete, Voutes Campus, Heraklion, Crete, GR-71003, Greece

ARTICLE INFO

ABSTRACT

This paper focuses on the effects of biological and synthetic polymers on the formation of amorphous silica. A concise review of relevant literature related to biosilicification is presented. The importance of synergies between polyelectrolytes on the inhibition of silicic acid condensation is discussed. A specific example of a zwitterionic polymer phosphonomethylated chitosan (PCH) is further analyzed for its inhibitory activity. Specifically, the ability of PCH to retard silicic acid condensation at circumneutral pH in aqueous supersaturated solutions is explored. It was discovered that in short-term studies (0–8 h) the inhibitory activity is PCH dosage-independent, but for longer condensation times (>24 h) there is a clear increase in inhibition upon PCH dosage increase. Soluble silicic acid levels reach 300 ppm after 24 h in the presence of 160 ppm PCH. Furthermore, the effects of either purely cationic (polyethyleneimine, PEI) or purely anionic (carboxymethylinulin, CMI) polyelectrolytes on the inhibitory activity of PCH is systematically studied. It was found that the action of inhibitor blends is not cumulative. PCH/PEI blends stabilize the same level of silicic acid as PCH alone in both short-term (8 h) and long-term (72 h) experiments. PCH/CMI combinations on the other hand can only achieve short-term inhibition of silicic acid polymerization, but fail to extend this over the first 8 h. PCH and its combinations with PEI or CMI affect silica particle morphology, studied by SEM. Spherical particles and their aggregates, irregularly shaped particles and porous structures are obtained depending on additive or additive blend. It was demonstrated by FT-IR that PCH is trapped in the colloidal silica matrix.

Contents

* Corresponding author.
   E-mail address: demadis@chemistry.uoc.gr (K.D. Demadis).
   URL: http://www.chemistry.uoc.gr/demadis (K.D. Demadis).

1. Introduction

Nature directs the formation of amorphous hydrated silica (biosilica) in living organisms, such as marine/freshwater diatoms and terrestrial plants via the important process of biosilicification [1–3]. One can put this in perspective by considering that the gross production of biogenic silica in surface waters was estimated to be ~240 ± 40 terramoles of silicon per year. This means, marine biological systems process the breathtaking amount of about 6.7 gigatonnes of silicon annually [4]. Biosilicification is a unique kind of biomineralization. Its uniqueness and differentiation from a plethora of other biogenic, metal-containing minerals (*e.g.* calcite, aragonite, vaterite, octacalcium phosphate, hydroxyapatite, iron sulfides, *etc.*) lies not only with the simple, albeit unique, structure of the final product, amorphous silicon dioxide (silica), but also with the intricate (and enigmatic) mechanism of its formation. Whereas metal carbonate and phosphate solids are crystalline ionic materials whose formation is governed by cation–anion association and solubility equilibria, silica is an oxide of amorphous nature formed by a complicated inorganic polymerization process that is controlled by organic macromolecules, resulting in "exotic" morphologies at the micron scale [5].

Silicon, in the form of silicic acid, is a fundamental nutrient not only for diatoms, but also for silicoflagellates, radiolaria, and many sponges, all of which polymerize it to build skeletons of biogenic silica. According to Maldonado et al. [6], our current understanding of the silicon cycle in the ocean assumes that diatoms dominate not only the uptake of silicic acid, but also the production and recycling of biogenic silica, and that other organisms with siliceous skeletons, including sponges, radiolarians, and silicoflagellates, play a negligible role. These authors showed that the retention of "Si" by siliceous sponges in some sublittoral and bathyal environments is substantial and that sponge populations function as "Si" sinks. Therefore, sponges may affect "Si" cycling dynamics and "Si" availability for diatoms, particularly in Si-depleted environments. It was strongly suggested by Maldonado that the role of sponges in the benthopelagic coupling of the "Si" cycle is significant. For example, Antarctic giant hexactinellids, such as *Rossella nuda* and *Scolymastra joubini*, which may be up to 2 m tall, 1.4 m in diameter, and up to 600 kg wet weight, containing up to 50 kg biogenic silica each.

Silica deposition is also a fundamental process in sponges. According to the modern point of view, two different mechanisms of silicification in sponges are proposed: enzymatic (silicatein-based) and non-enzymatic, or self-assembling (chitin- and collagen-based). There are two possible mechanisms for enzyme catalysis [7]: (i) stabilization of one molecule of deprotonated silicic acid (the nucleophile) at the active site, which will then react with another molecule of silicic acid; or (ii) stabilization of a protonated silicic acid (the electrophile) which will then react with another molecule of silicic acid.

Silicon was found associated with glycosaminoglycans bound as an ether or ester-like silicate with $C-O-Si$ or $C-O-Si-O-Si-O-C$ bonds, in amounts of one Si atom/130–280 repeating units of the organic [8]. Recently, Ehrlich et al. isolated and identified chitin from skeletal formations of some marine glass sponges for the first time. The presence of chitin within the framework skeleton of *Farrea occa* [9] and *Euplectella aspergillum* [10] as well as separate spicules *Rossella fibulata* [11] could also be revealed by gentle NaOH-based desilicification technique established by Ehrlich et al. [12,13]. It was suggested that silicate ions and silica oligomers preferentially interact with glycopyranose rings exposed at the chitin surface, presumably by polar and H-bonding interactions [14].

Furthermore, Ehrlich et al. reported recently and for the first time an example of *Hyalonema sieboldi* glass sponge whose spicules are a biocomposite containing a silicificated collagen matrix. The high collagen content is the origin of the unique mechanical flexibility of the spicules [12,13].

2. Macromolecules that affect silicification

The *in vivo* process of silicic acid condensation to yield silica nanopatterns is profoundly influenced by complex organic biomolecules. These, (mainly studied in sponges and diatoms) play an integral and complicated role in biosilica morphosynthesis [15,16]. Insight into the nature of this intricate organic matrix has been realized through characterization of diatom biosilica-associated peptides (silaffins, natSil-1 and natSil-2) and long-chain polyamines (LCPA) [17]. Silaffins contain repeated peptide sequences that are rich in basic amino acids (lysine and arginine) and unusual alkylamine post-translational modifications, see Fig. 1.

Silaffins assist in the formation of the silica wall that encompasses the diatom [18]. Furthermore, it has been suggested that formation of organic matrices composed of polyanionic natSil-2-like phosphoproteins and polycationic silica-forming components may represent a widespread mechanism in diatom biosilica morphogenesis [19].

Morse and coworkers have extensively studied the silica-producing proteins, silicateins, derived from sponge spicules. Through point mutation studies, histidine and serine were identified as the catalytic component in the active site of the protein [20]. Silaffins, isolated from *Cylindrotheca fusiformis*, have been shown to form silica at pH ~5.5. Structural analysis of one such silaffin, NatSil1A, revealed that serine residues were phosphorylated and the lysine were post-translationally modified forming N-dimethyl-lysine, N-trimethyl-hydroxy-lysine, and long-chain polyamines, derivatives of polypropylenimine [21].

HF-based extraction experiments allowed the isolation of three silaffins [22]. Two of them, the silaffin-1A1 and silaffin-1A2, were sequenced by mass spectrometry and were shown to be encoded by the same sil1 gene from *C. fusiformis* [23]. These silaffin-1A peptides are enriched in lysine and serine groups. Moreover, amino groups of the lysine residues are modified by introduction of long-chain polyamines, N,N-dimethyl-lysine or N,N,N-trimethyl-hydroxy-lysine. Another fraction of methylated polyamines were also recovered and identified from a HF extraction procedure [24]. When put in contact with HF extracts, aqueous solutions of prehydrolyzed silicon alkoxides at pH 7 form and precipitate silica nanoparticles.

Of particular interest is the fact that, at pH ~5, unsubstituted polyamines did not induce silica formation, whereas alkylated ones did. This is to be linked with previous reports on a possible acid pH within the Silica Deposition Vescicle (SDV) [25–28]. More recently, HF treatment in milder conditions revealed that the hydroxy groups of the silaffin serine residues were phosphorylated, illustrating the possible degradation of pristine molecules during the initial extraction process [20–22]. These zwitterionic proteins exhibit self-assembly properties that may be involved in the frustule morphogenesis [29].

In addition to silaffins, a biomimetic analogue derived from a repeat unit of the Natsil gene, the R5 peptide (SSKKSGSYSGSKGSKRRIL), induces precipitation of silica from monosilicic acid [30]. Mutation studies of the R5 peptide have shown that the RRIL motif is critical for silica formation, as it causes the peptide to self assemble, providing a locally high amine concentration, and promoting the subsequent condensation of monosilicic acid. Moreover, diatoms also contain long-chain polyamines such as N-methylated poly(propylene imines) attached to putrescine cores that are capable of precipitating silica [31].

The discovery that positively charged biomacromolecules (zwitterionic to be precise) can direct biosilica synthesis *in vivo* and *in vitro* was followed by a battery of research efforts to discover and test synthetic
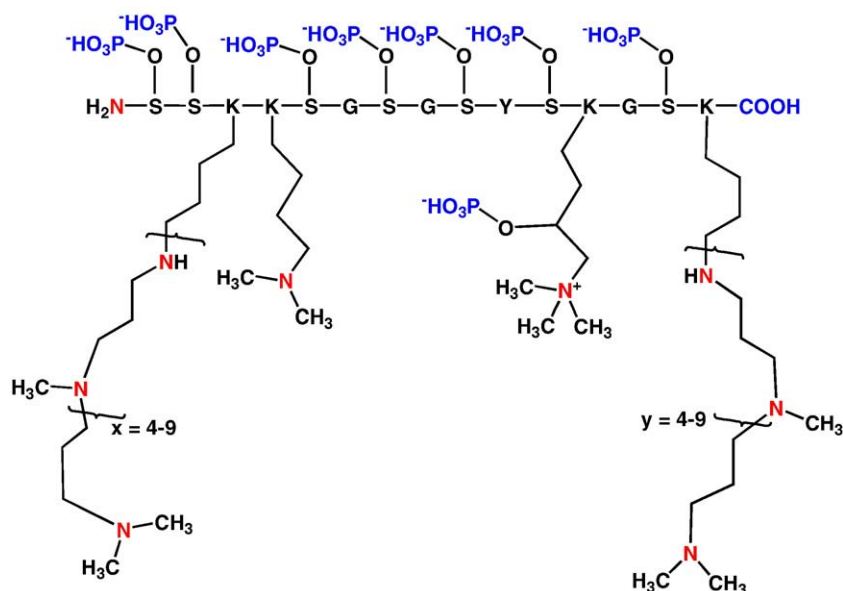
Fig. 1. Schematic structure of silaffin 1-A1 from *Cylindrotheca fusiformis* cell walls treated with hydrofluoric acid (HF), showing modified lysine groups and phosphorylated hydroxyl groups. The presence of N groups that could potentially acquire cationic charge (red) and anionic moieties (phosphates, blue) is highlighted. The polypeptide is represented in the one-letter amino acid code (S = serine, K = lysine, G = glycine, Y = tyrosine). Adapted from Ref. [23]. (For interpretation of the references to color in this figure legend, the reader is referred to the web version of this article.)

polymers and their effects on silicic acid polymerization *in vitro* [32]. The cationic polymer template assembles the silicic acid species through electrostatic interactions and hydrogen bonding. This interaction results in the aggregation and subsequent condensation to form silica [33–35]. Some representative examples are given below, but further cases will be examined in a later section of this manuscript.

Patwardhan et al. have investigated the ability of poly-L-lysine [36], as well as a variety of other cationic polymers such as poly-L-histidine [37], polyallylamine [38], poly-L-arginine [39], polyethyleneimine [40] and amine-terminated polyaminoamide dendrimers [41] to form silica from monosilicic acid *in vitro*.

Simmons et al. have studied the effects of a plethora of amine/ ammonium compounds on silicic acid condensation to form colloidal silica [42]. Among the compounds studied were various mono-ammonium salts, *bis*(quaternary ammonium) salts, highly alkylated diamines, *etc.*, in phosphate-buffered silicic acid aqueous solutions. It was discovered that the degree to which a series of diamines in solution enhances condensation of silicic acid at neutral pH increases with increasing alkylation, a factor more important than amine pK_a. These observations support a previously proposed mechanism in which neighboring cationic amines "force" silicate oligomers into a configuration favoring condensation. Also, amines with a high degree of alkylation showed enhanced silicic acid condensation kinetics. Similar studies with a variety of amines, but using water-soluble silicates, were carried out by Menzel et al. [43]. Jones et al. studied the effect of various compounds on tetraethylorthosilicate (TEOS) condensation, such as 1,4-diazabicyclo {222}octane (DABCO), imidazole and pyridine and their derivatives, by monitoring gelation times [44]. Perry et al. synthesized linear poly (propylamines) in an effort to extend the N-methylpropylamine chain in a linear fashion, and then studied the effects of these molecules on silica formation [45]. Neutral $H_2N(CH_2)_nNH_2$ bolaamphiphiles ($n = 12$–22) were studied as structure directors in TEOS hydrolysis to produce a family of silica molecular sieves with lamellar frameworks and hierarchical structure [46]. Furthermore, a series of ionene polyviologens were synthesized and incorporated into silica networks prepared by the sol-gel route based on TEOS hydrolysis [47]. Lastly, surfactant-influenced, directed growth of silica hollow spheres were studied. Compounds tested were mixtures of cetyltrimethylammonium bromide (CTAB) and sodium

perfluorooctanoate (FC7) and also mixtures of cetyltrimethylammonium tosylate (CTAT) and sodium dodecylbenzenesulfonate (SDBS) [48].

Silicon bio-transport (*i.e.* silicic acid transport and pre-concentration prior to silica formation) is an integral part of biosilicification. Within the diatom cell relatively high silicic acid levels must be maintained for a period of time before its condensation to form amorphous silica [49–52]. In fact, silicate ionophoretic compounds have been isolated from the diatom [53], suggesting an intracellular transport mechanism occurring by ionophore-mediated diffusion [54]. The previously proposed Silica Transport Vescicles (STV's) [49–53] were never shown to contain any "Si cargo", so their role in biosilica formation has been suggested to be delivery of membrane parts to the expanding SDV.

Silicic acid condensation follows a precisely chosen pathway in Nature to yield preferred nanopatterned structural motifs and architectures [55]. There are several other scientific areas, where silicates and silica play a central role, such as geochemistry [56,57], general medicine [58], orthopaedics [59], nutrition [60,61], cement technology [62], nanoparticle technology [63], water treatment [64], and others. Scientists working at the interface of different research areas have been utilizing each other's knowledge and expertise, not only to get deeper insight into complex biochemical processes involved in natural systems, but also to design novel materials that may be biomimetic analogs of complex systems found in Nature.

An important engineering application is water chemical technology. In supersaturated silica-laden process waters silicic acid polymerizes *via* a condensation polymerization mechanism, just like in Nature, at appropriate pH regions [65,66]. The resulting amorphous silica precipitate, after Ostwald ripening [67], is slowly converted into a hard and tenacious deposit on critical industrial equipment components, such as heat exchangers, transfer pipes, *etc.* Since silica removal by dissolution is a challenge both from an environmental and safety perspective [68,69], commonly practiced control approaches have been limited to: (a) maintaining undersaturation (leading to water wastage), (b) pre-treatment (with high capital/equipment costs) and (c) inhibition of silica/silicate formation by chemical additives. The latter approach is practiced by some water service industries, with partial success [70].

Our on-going research efforts in the (bio)silicification area focus on the inhibitory effects of polymeric molecules on colloidal silica formation by studying the stabilization of silicic acid by these polymers [71–78]. In a biomimetic approach we utilize information available on biomacromolecule-induced biosilica formation in order to design, synthesize and utilize macromolecules that may have inhibitory activity on colloidal silica formation, thus extending the life of soluble silicic acid prior to its self-condensation to form colloidal silica.

We have selected to utilize chitosan-based biopolymers [79,80], Fig. 2, as additives that may stabilize silicic acid and delay its self-condensation to yield amorphous silica. More specifically, in this paper we study the polymer chitosan on which animomethylenepho-sphonate groups have been grafted by a Mannich-type reaction [81]. We selected this particular polymer because it possesses attractive similarities to silaffins, among other reasons outlined below. In particular: (a) PCH possesses cationic charge by virtue of its protonated (at pH 7) $-NH_3^+$ groups, (b) PCH possesses anionic phosphonate groups (deprotonated $-PO_3H^-$ or $-PO_3^{2-}$ moieties) that resemble the phosphate groups in silaffins, (c) PCH contains tertiary and secondary, protonated amine groups (from the aminomethyle-

nephosphonate moiety), also present in silaffins. Furthermore, PCH is synthesized from chitosan (a degradation product of chitin, a renew-able material) in an efficient and low-cost manner. PCH also has low aquatic toxicity (vide infra). An additional reason that prompted us to study the effect of PCH on silicic acid condensation is the report that the diatom cell wall (frustulum) is made of nanostructured amorphous silica that is associated with polysaccharides and proteins [48,82,83]. The link that may exist between polysaccharides and the formation of biosilica seems to be an interesting area to explore. We are aware of evidence that some diatoms produce extracellular chitin (a PCH precursor), and that there is no proof that chitin-like biomolecules are present inside diatom cells [9–14]. Therefore, the approach followed herein is an attempt to "model" silicic acid "pre-concentra-tion" in vitro, just prior to its condensation yielding colloidal silica, or essentially to delay silicic acid condensation. In addition, we attempt to explore the possible synergies between zwitterionic PCH with either purely cationic polyethyleneimine (PEI), or purely anionic carbox-ymethylinulin (CMI) and their effects in silicic acid stabilization. Our initial results with PCH were recently published and some of them are used herein only for comparison purposes [78].
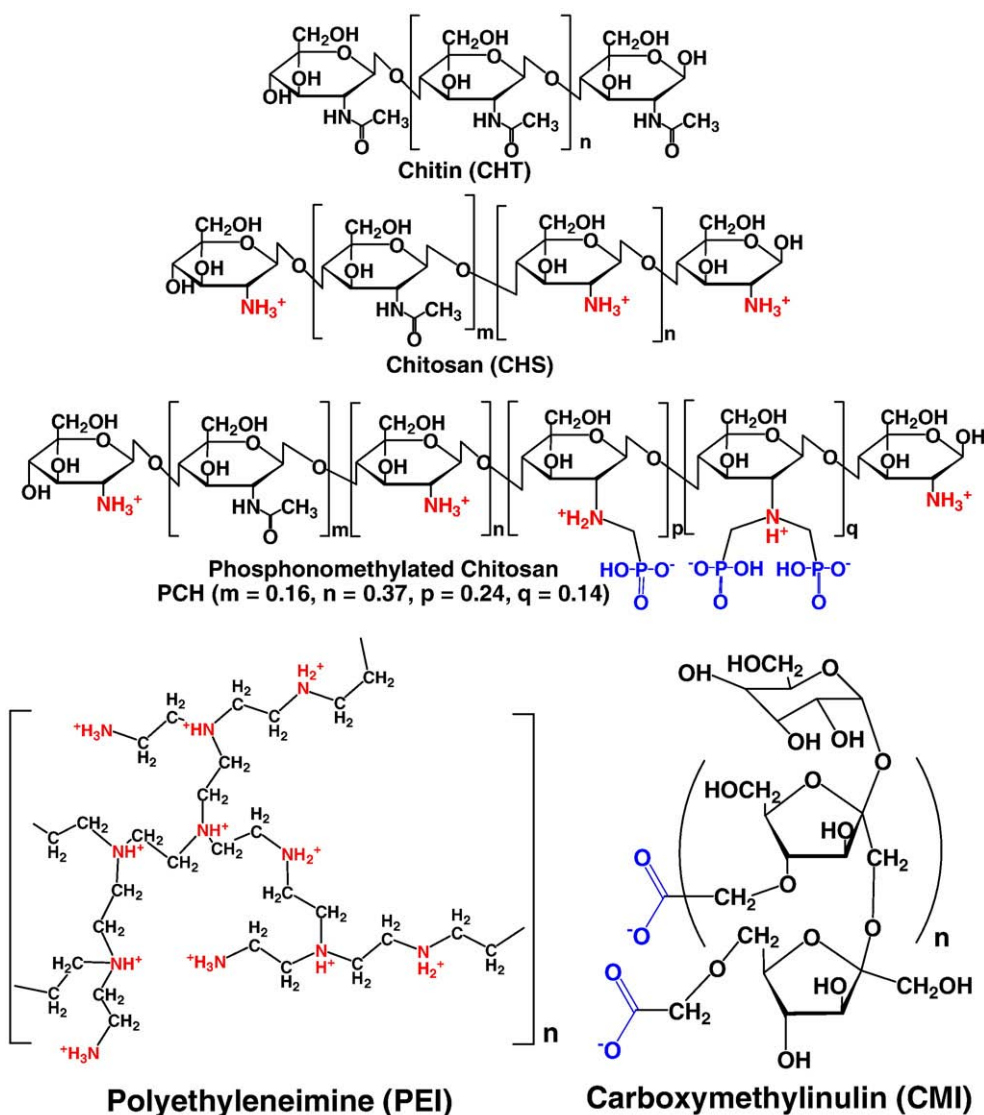

Fig. 2. Schematic structures of chitin (CHT), chitosan (CHS), phosphonated chitosan (PCH), polyethyleneimine (PEI) and carboxymethylinulin (CMI). Cationic groups are highlighted in red, anionic in blue. (For interpretation of the references to color in this figure legend, the reader is referred to the web version of this article.)

3. Experimental protocols

3.1. Instrumentation

IR spectra were recorded on a FT-IR Perkin–Elmer FT 1760. Measurements of soluble silicic acid were carried out using a HACH 890 spectrophotometer from the Hach Co., Loveland, CO, U.S.A. SEM images were collected on a scanning electron microscope LEO VP-35 FEM.

3.2. Materials

Schematic structures of the polymers used in this study are shown in Fig. 2. Polyethyleneimine (PEI, branched, MW 70 kDa, ~25% primary amines, ~50% secondary amines and ~25% amines) was from Polysciences. PCH was synthesized according to published procedures [84–86]. CMI, carboxymethylinulin, (proprietary MW, between 2 and 3 kDa) was from Solutia Inc. (Belgium). CMI can be prepared from the biopolymer inulin via a carboxymethylation step [87]. Sodium silicate $Na_2SiO_3 \cdot 5H_2O$, ammonium molybdate $((NH_4)_6Mo_7O_{24} \cdot 4H_2O)$, and oxalic acid $(H_2C_2O_4 \cdot 2H_2O)$ were from EM Science (Merck). Sodium hydroxide (NaOH) was from Merck, hydrochloric acid 37% was from Riedel de Haen.

Acrodisc filters (0.45 µm) were from Pall–Gelman Corporation. In-house, deionized water was used for all experiments. This water was tested for soluble silica and was found to contain negligible amounts. Molecular weight determination for PCH was performed by viscosity analysis of a PCH aqueous solution. The solvent system used was 0.3 M acetic acid/0.2 M sodium acetate. The values for the Mark–Houwink equation "K" and "a" constants were 1.81×10^{-2} and 0.93, respectively. Viscosity measurements were made on an Ubbelohde viscometer (Schott Geräte TYP 52520/II). The average molecular weight was found ~254 kDa. Solid PCH was also studied by SEM and the images are shown in Fig. 3.

3.3. Toxicity protocols

A facile model system to study human disease and drug responses are zebrafish, *Danio rerio*. They are particularly suited for this purpose because they represent a vertebrate species, their genome is sequenced, and a large number of synchronously developing, transparent embryos can be produced. Zebrafish embryos are permeable to drugs and can easily be manipulated using well-established genetic and molecular approaches [88,89]. LC₅₀ values (50% lethal concentration) is the concentration at which 50% of test organisms are killed. Adult wild-type zebrafishes were maintained at 26 °C and fed with ZF Biofood. Fertilized zebrafish embryos were obtained by hormonally induced treatment to spawners and *in vitro* fertilization. Three assays with a variable number (4–7) of water soluble-N-methylene phosphonic chitosan concentrations between 99 and 1000 mg/l and a control

without N-methylene phosphonic chitosan were conducted in 96-well multiplates at 26 °C. Spawns and eggs were selected at 3–4 hpf (hours post-fertilization) according to standard criteria. Lethal effects were observed in 48 hpf embryos, based on four morphological and functional endpoints, specific for lethality studies. The LC_{50} of N-methylene phosphonic chitosan was determined in our laboratory using the Probit 1.5 software as 279.6 ± 29.7 mg/L. The LC_{50} of chitosan was reported as 300 ± 18 mg/l and in our case the phosphonomethylated chitosan derivative (PCH) 280 ± 30 mg/l. The PCH polymer tested presents a LC_{50} value similar to chitosan (CHT), indicating that *phosphonomethylation does not enhance toxicity*.

3.4. Methods

The protocols for all experiments and measurements described herein have been reported in detail elsewhere [90]. Molybdate-reactive silicic acid was measured using the silicomolybdate spectrophotometric method [91–95], which has a $\pm 5\%$ accuracy. Reproducibility was satisfactory. Briefly, the procedures are outlined as follows.

3.5. Silicic acid supersaturation protocol ("control")

100 mL from the 500 ppm (as SiO_2) or 8.33 mM sodium silicate stock solution was placed in a plastic container which contained a teflon — covered magnetic stir bar. The pH of this solution was initially ~11.8 and adjusted to 7.00 ± 0.1 by addition of HCl or NaOH, if needed (9 drops of conc. HCl (10%) and then another 9 drops of dilute HCl (5%). The volume change was taken into account in calculations). Then the container was covered with plastic membrane and set aside without stirring. The solutions were checked for soluble silicic acid by the silicomolybdate method every hour for the first 8 h (short-term experiments) or after 24, 48, 72 h (long-term experiments) time intervals after the pH adjustment to 7.00.

3.6. Protocol for the effect of additives on silica formation

100 mL portions of the 500 ppm (as SiO_2) or 8.33 mM sodium silicate stock solution were placed in PET containers charged with teflon-covered magnetic stir bars. In each container different volumes of inhibitor (10,000 ppm stock solution) were added to achieve desirable inhibitor concentration. This stock solution concentration is convenient for simple inhibitor additions to the working solutions. For example, if a dosage of 40 ppm inhibitor is needed, then 0.4 mL of the stock solution is added. After that the same procedure for the control test was followed.

3.7. Quantification of "soluble (reactive) silica"

"Soluble or reactive silica" actually denotes soluble silicic acid and was measured using the silicomolybdate spectrophotometric method.
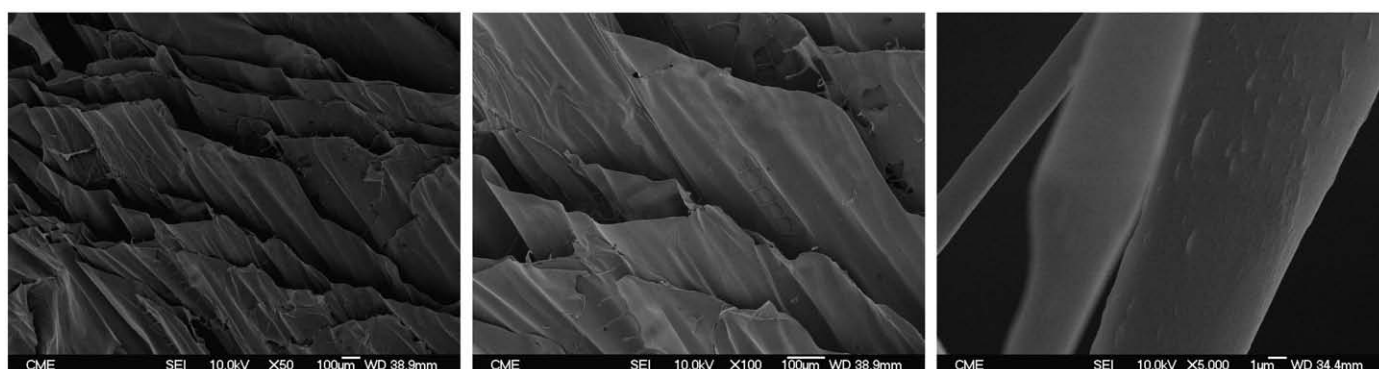

Fig. 3. SEM images of solid PCH morphology used in this study.

According to this method 2 mL filtered sample, with 0.45 μm syringe filter, from the test solution is diluted to 25 mL in the cell, with light path 1 cm. 1 mL ammonium molybdate stock solution and 0.5 mL 1 + 1 HCl are added to the sample cell, the solution is mixed well and left undisturbed for 10 min. Then 1 mL oxalic acid solution is added and mixed again. The solution is set aside for 2 min. After the second time period the photometer is set at zero absorbance with water. Finally the sample absorbance is measured at 452 nm as "ppm soluble silica". The detectable concentrations range is 0–75.0 ppm. In order to calculate the concentration in the original solution a dilution factor is applied. The silicomolybdate method is based on the principle that ammonium molybdate reacts with reactive silica and any phosphate present at low pH (about 1.2) and yields heteropoly acids, yellow in color. Oxalic acid is added to destroy the molybdophosphoric acid leaving silicomolybdate intact, and thus eliminating any color interference from phosphates. It must be mentioned that this method measures "soluble silica" and in this term includes not only the monomer silicic acid but also oligomer species such as dimers, trimers, tetramers, *etc.* It is not stated exactly which are the reactive units. It should be noted that all additives tested in the present paper do not interfere with the silicomolybdate spectrophotometric method.

4. Results

Our research efforts have been focusing on utilization of "natural" or "synthetic" polymeric additives that influence (inhibit or direct) colloidal silica formation. In particular, we have placed significant attention on: (a) the inhibitory effect that polymeric additives have on silica precipitate formation, while they delay silicic acid polymerization (b) the use of non-toxic, environmentally friendly, "green" chemical additives that can enhance silicic acid solubility (c) exploiting the significant observation (by other research groups and us) that cationic additives have profound effects on silica particle formation and (d) delineating various process variables that may affect additive effectiveness, notably, minimizing polymer dosage while maximizing inhibitory performance.

We recently reported utilization of polyaminoamide-based (PAMAM) dendrimers as inhibitors of silica formation, particularly those that are amine-terminated [71–78,90]. Although these dendrimeric additives are effective silica growth inhibitors, their relatively high cost at present has prompted efforts to discover new, more cost-effective and more effective additives as possible replacements. Therefore, alternative, lower cost chemical approaches need to be sought while maintaining high inhibitory efficiency. In accord with several literature reports, the extent to which a chemical additive (polymeric or monomeric) influences silica growth depends on a certain (not yet precisely identified) degree of cationic charge on the molecule backbone. This cationic charge is also necessary for inhibitory activity on silica formation, as well. However, it should be noted that "small" cationic species (such as H_4N^+ or Et_4N^+) are not effective silica inhibitors at levels up to 200 ppm [96]. In contrast, literature reports show that small molecules with functional groups possessing cationic charge, such as proline, lysine, aspartate and serine, exert some, albeit minor, catalytic effect on silicic acid condensation [97]. Amine-terminated PAMAM dendrimers at low dosages (40 ppm is the optimum) stabilize silicic acid, but at the same time, due to their cationic charge from protonated surface amine groups at pH 7 [98,99], interact with anionic colloidal silica particles (originating from the inability of the dendrimer to achieve quantitative inhibition) to form PAMAM-SiO$_2$ composite precipitates. The propensity of the dendrimeric inhibitor to be entrapped within the silica 3D matrix is alleviated by addition of anionic polyelectrolytes (*e.g.* polyacrylates and related polyelectrolytes) that, in part, neutralize excessive cationic charge on the cationic polymer. This approach, although successful, requires utilization of two separate,
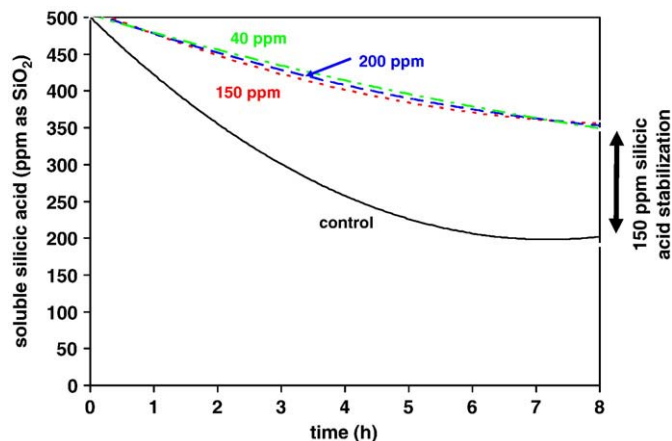

Fig. 4. Effect of PCH levels on colloidal silica inhibition in short-term (8 h) experiments.

oppositely charged macromolecules. Therefore, a strategy that involves a zwitterionic polymeric additive that would combine both positive and negative charge in the same polymeric backbone, would be preferable. Although the accelerating effect of cationic macromolecules on silica formation is well established, the effect of zwitterionic macromolecules has been much less studied. Notably, small peptides have been reported to accelerate silica formation in vitro, but no effects on stabilization of silicic acid were noted [100,101]. The use of PCH, a zwitterionic polymer, that is derived from renewable sources acts as an effective inhibitor of colloidal silica formation. Below, results are presented on the inhibitory effects of PCH alone, and in combination with a purely cationic (PEI) polymer or a purely anionic (CMI) polymer.

4.1. Silica formation in the presence of phosphonomethylated chitosan (PCH)

Phosphonomethylated chitosan (PCH) was tested for its ability to stabilize silicic acid and influence amorphous silica formation in "short-term" experiments (8 h) at dosages 40, 150 and 200 ppm. The results are presented in Fig. 4. Silicic acid condensation appears to be independent of additive dosage within the first 8 h. Soluble silicic acid reaches a value of ~350 ppm after 8 h. Compared to control solutions not containing PCH this results in ~150 ppm additional silicic acid stabilization.

The long-term silicic acid stabilization by PCH was studied over a 72 h time period with sampling every 24 h. The effect of various dosages of PCH (10, 20, 40, 60, 100, 150 and 200 ppm) on silica formation is shown in Fig. 5. An immediate observation is that PCH can only delay
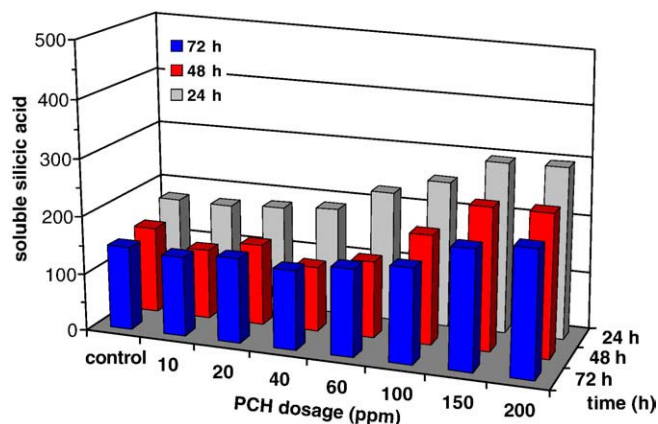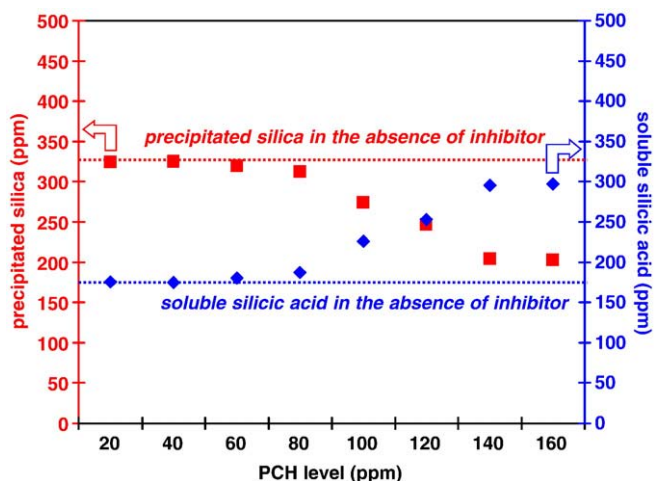

Fig. 5. Stabilization of silicic acid in the presence of PCH in long term (24–48–72 h) experiments.
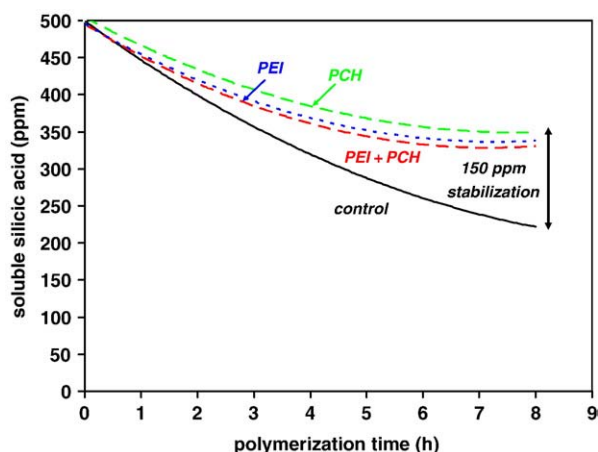
Fig. 6. Stabilization of silicic acid (right *y*-axis) and colloidal silica precipitation (left *y*-axis). The measurements were taken after 24 h of condensation time.

Fig. 8. Effect of PCH dosage (20–40–60 ppm) with constant PEI dosage (20 ppm) on colloidal silica inhibition in "long-term" experiments.
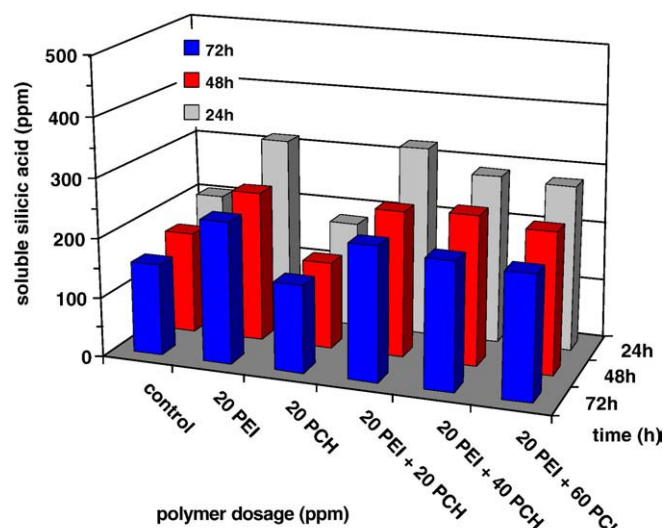
silicic acid condensation over the course of 72 h, thus only partially inhibiting silica formation. These experiments reveal that there is a dosage-dependence (in contrast to 8-hour experiments) on silicic acid stabilization that reaches a maximum at 150 ppm PCH (296 ppm silica compared to 176 ppm of the "control"). This translates to 120 ppm silicic acid stabilization (over the control) for the first 24 h. Low dosages (10 and 20 ppm) exhibit virtually no long-term inhibitory effects. There seems to be a sharp reduction in inhibitory action after 24 h. This has been observed numerous times in our experiments with a variety of additives. Specifically, for the 150 ppm dosage, there is a 50 ppm drop in silicic acid levels between 24 h and 48 h. The same is true for the 200 ppm dosage.

As will be discussed extensively later, a reason for the reduction in inhibitor activity is PCH entrapment in the colloidal silica matrix, as will be discussed later. This results in unavailability of sufficient PCH in solution to continue inhibition and in further drop in silicic acid levels.

The above experiments demonstrate that PCH can only partially inhibit silicic acid condensation, thus amorphous silica forms as a "fluffy" precipitate in the reaction vessels. The precipitate was collected and weighted. Fig. 6 relates the dosage-dependent inhibition of silicic acid (right axis) and silica precipitation (left axis). The measurements were taken after 24 h of condensation time.

4.2. Silica formation in the presence of phosphonomethylated chitosan (PCH) and cationic polyethyleneimine (PEI) mixtures

The inhibitory effects of combinations of PEI and PCH were tested in silicic acid polymerization. The "short-term" and "long-term" results are shown in Figs. 7 and 8, respectively. In spite of its profound structural differences to PCH, the inhibitory action of PEI (20 ppm) appears to be comparable to that of PCH (40 ppm), with only minor differences. PEI is only slightly less active than PCH within the first 4 h of condensation. Addition of PEI and PCH combinations to silicic acid solutions give also marginal differences in performance, compared to that of PEI alone, or PCH alone. It is noteworthy that there appears to be no discernible synergy between the two additives for inhibitory activity enhancement. Furthermore, the effect of PEI and PCH (when both present in solution simultaneously) is not cumulative. If that were the case then PEI (at 20 ppm dosage) and PCH (at 40 ppm dosage) should inhibit silica formation quantitatively, reaching 500 ppm soluble silica. The results show that ~350 ppm remains soluble when the above combination of inhibitors is present (Fig. 7).

This observation demonstrates the interaction of PEI and PCH in solution, presumably due to an electrostatic attraction and/or hydrogen bonding between the anionic phosphonate groups on the PCH backbone and the protonated, cationic amine groups on the PEI [102]. The resulting "combined" dual polymeric inhibitor formed by polyanion–polycation association does not exhibit any enhanced inhibitory activity, compared to that of its components, PEI and PCH. Long-term silicic acid polymerization studies further confirm these results. This should be contrasted to observations noted on increased inhibitory activity of combinations of cationic PAMAMs and poly-anionic electrolytes, such as carboxylate-based polymers [76]. Fig. 8 shows that addition of 20 ppm of PEI to solutions containing 20 ppm PCH has virtually no beneficial effect on inhibitory activity of 20 ppm PCH. Further PCH dosage increase (up to 60 ppm), while maintaining 20 ppm PEI dosage has actually a small but measurable detrimental effect.

4.3. Silica formation in the presence of phosphonomethylated chitosan (PCH) and anionic carboxymethylinulin (CMI) mixtures

It is well established that anionic polymers do not affect silicic acid polymerization. There is only one report in the literature of the inhibitory activity of a genuinely anionic polymer, phosphinopoly-carboxylic acid (PPCA, a polyacrylate-based polymer), causing
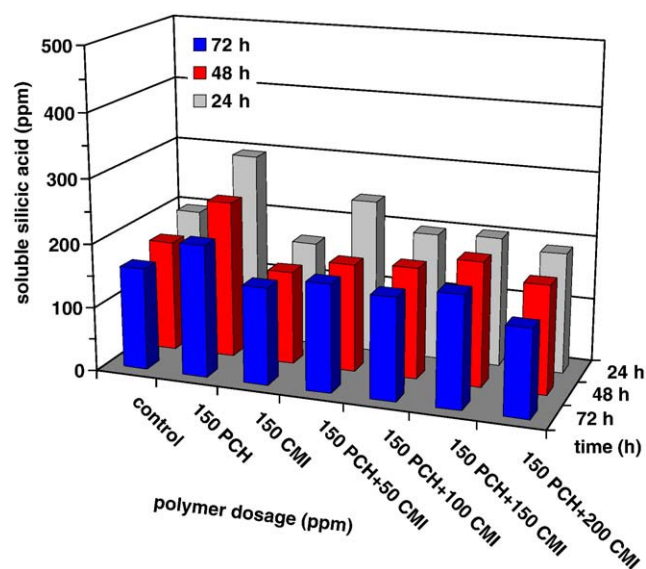

Fig. 7. Synergistic action of PEI and PCH in colloidal silica inhibition in "short-term" experiments. PEI, 20 ppm dosage; PCH, 40 ppm dosage.

Fig. 9. Effect of CMI dosage (0–50–100–150–200 ppm) with constant PCH dosage (150 ppm) on colloidal silica inhibition in long-term experiments.

stabilization of 325 ppm soluble silicic acid, albeit at very high dosage (1000 ppm) [103]. CMI alone does not affect silicic acid condensation at dosage levels up to 200 ppm (see third set of bars in Fig. 9).

We recently reported that CMI can enhance the inhibitory activity of PCH at <8 h silicic condensation times, when the two polymers act in combination in solution (50 ppm PCH and >50 ppm CMI) [78]. In this context, we investigated whether this beneficial synergy has a life-time beyond 8 h. Thus, when PCH is combined with CMI in "long-term" silicic acid condensation experiments, a substantial reduction in its inhibitory activity is noted, see Fig. 9.

Addition of 50 ppm CMI to 150 ppm PCH causes a 100 ppm (from 342 to 241 ppm) reduction in silicic acid stabilization after 24 h polymerization time. Further CMI dosage increase to 100 ppm results in complete "deactivation" of PCH's inhibitory activity. Additional CMI dosage increase exerts no further effects, as silicic acid levels are identical to the "control" experiment. The observed detrimental effects on PCH inhibitory activity are somewhat expected. Similar observations have been noted on the effect of polyanionic polymers (polyacrylate, poly(acrylamide-co-acrylate) and CMI) on amine-terminated, cationic polyaminoamide (PAMAM) dendrimers [104].

4.4. The effect of ionic strength on the efficiency of inhibitors

The profound effect of salinity on biosilica formation has been noted for the two marine diatom species *Thalassiosira punctigera* and *Thalassiosira weissflogii* [105]. It was discovered that diatom biosilica appears to be denser when formed at the lower salinity used. This phenomenon was explained by assuming aggregation of smaller coalescing silica particles inside the silica deposition vesicle, which would be in line with principles in silica chemistry [106,107]. Iler has reported that the presence of metal cations can accelerate silica formation and reduce gelation times, due to the coagulating effect of the positive charge on the negatively charged particles [65]. To the best of our knowledge there is no systematic study in the literature on the effects of ionic strength on the action of silica inhibitors. However, Lindberg et al. have reported that increased salt concentration (NaCl) results in an increase in silica particle size (synthesized from TEOS hydrolysis) [66]. Therefore, we feel that presenting some initial results herein in relation to the effects of PCH and its blends with CMI is warranted.

In Fig. 10 the effect of 0.5 M NaCl on silicic acid polymerization without (control) and with inhibitors (PCH and PCH/CMI combinations) is shown. The effect of NaCl on pure silicic acid condensation (control) is
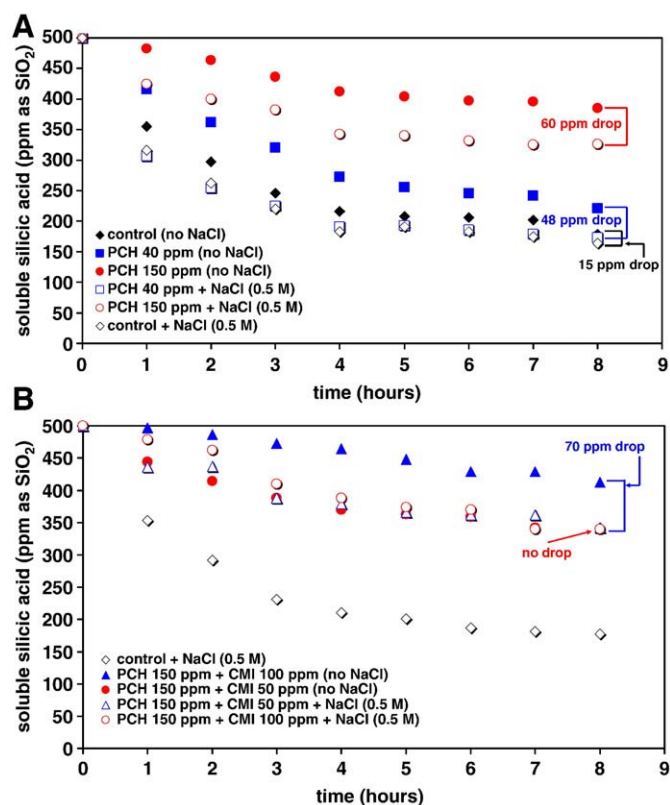

Fig. 10. The effect of 0.5 M NaCl on the inhibitory action of PCH and PCH/CMI mixtures. For graph A: full points (rhombs, squares and circles) refer to polymerization of silicic acid without 0.5 M NaCl; void points refer to polymerization of silicic acid in the presence of 0.5 M NaCl. Black colored rhombs refer to the "control" (with or without NaCl); blue colored squares refer to solutions containing 40 ppm PCH (with or without NaCl); red colored circles refer to solutions containing 150 ppm PCH (with or without NaCl). For graph B: full points (rhombs, squares, circles and triangles) refer to polymerization of silicic acid without 0.5 M NaCl; void points refer to polymerization of silicic acid in the presence of 0.5 M NaCl. black colored rhombs refer to the "control" with NaCl; blue colored triangles refer to solutions containing 150 ppm PCH and 100 ppm CMI (with or without NaCl); red colored circles refer to solutions containing 150 ppm PCH and 50 ppm CMI (with or without NaCl). (For interpretation of the references to color in this figure legend, the reader is referred to the web version of this article.)

minor. After 8 h of polymerization time there is only a 15 ppm drop in soluble silicic acid (graph A). If 40 ppm PCH is present the effect of NaCl is to reduce soluble silicic acid by 48 ppm and the inhibitory action is virtually diminished.

At a 150 ppm PCH level, the NaCl effect results in 60 ppm drop in soluble silicic acid (~380 ppm after 8 h), however the inhibitory efficiency is still high.

The effect of NaCl on the inhibitory action of PCH/CMI mixtures depends on CMI level (Fig. 10 B). For the 150 ppm PCH/50 ppm CMI combination the NaCl effect is essentially negligible. For the 150 ppm PCH/100 ppm CMI combination a drop of 70 ppm in silicic acid stabilization is noted (from 412 to 342 ppm). This can be possibly explained by the coordination ability of the carboxyl groups of CMI that are still free from any association with the ammonium groups of the PCH.

Such coordination and possible bridging between separate polymeric chains of CMI may cause further aggregation of silica particles. As will be seen later, PCH/CMI combination cause additional aggregation of silica particles.

4.5. Characterization of colloidal silica precipitates

There are several reports in the literature on the effects of various cationic polymers on silica precipitate morphology. In most cases, silica particles acquire the expected spherical particle features,
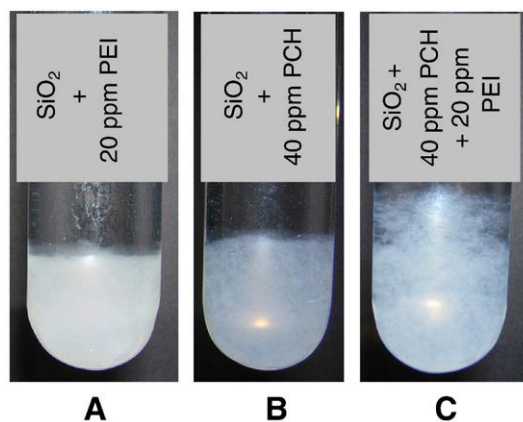
Fig. 11. Effect of PEI, PCH and PEI/PCH blend on silica precipitate macroscopic morphology. Photographs were taken after 8 h silicic acid polymerization.

although some other morphologies (platelets, hexagons, porous aggregates, etc.) have also been observed [108]. We have characterized the produced silica precipitates by FT-IR, optical photography, and SEM.

Visual inspection of the silica precipitates in the presence of PCH or its combinations with PEI or CMI give valuable information. Representative images are given in Figs. 11 and 12. Fig. 11 presents silica precipitates after 8 h condensation time in the presence of

20 ppm PEI, 40 ppm PCH and their combination. In the presence of 20 ppm PEI the silica precipitate appears amorphous, fluffy, non-compact and heavily hydrated (image A). PCH (40 ppm) precipitates colloidal silica that also looks fine and non-compact (image B). When PEI and PCH are used together, the silica precipitate appears less compact and less dense (image C).

It should be noted that in the presence of PEI (at 20 ppm), PCH (at 40 ppm) and PEI + PCH (20 + 40 ppm), essentially the same levels of silicic acid remain soluble after 8 h (see Fig. 6). However, the macroscopic properties of the silica precipitates differ to an appreciable extent. These macroscopic, visual observations are confirmed by the SEM studies (vide infra).

Changes in amorphous silica precipitates that result from solutions containing combinations of PCH and CMI are more dramatic (Fig. 12). The images in Fig. 12 were taken after 24, 48 and 72 h of silicic acid condensation time. PCH (150 ppm) causes precipitation of silica in a form of a fluffy, white precipitate. The amount of precipitate increases in time, as shown in the first row of photographs (images 1A, 1B, 1C). This is consistent with the reduction of soluble silicic acid levels observed in Figs. 5 and 6. When PCH (150 ppm) is used in combination with CMI (50 ppm) the morphology of the silica precipitates changes profoundly (images 2A, 2B, 2C).

The precipitates appear less fluffy, more compact and much less dispersed. The quantity of the precipitated silica also appears slightly higher. This is consistent with the results presented in Fig. 9, where addition of CMI (50 ppm) to solutions containing PCH (150 ppm) induce loss of 73 ppm soluble silicic acid (from 241 at 24 h to 168 ppm at 48 h). Increase of CMI levels (from 50 to 100 ppm) causes slight increase of the amount of silica precipitate (images 3A, 3B, 3C), in concert with the results (Fig. 9) that the silicic acid levels drop slightly. Finally, increase of CMI levels to 150 ppm induce the precipitation of less silica (at the bottom of the tube), but the supernatant appears more turbid, indicating the formation of much smaller silica particles that remain dispersed.

Examination of the silica precipitates by SEM was more informative (Fig. 13).

In "control" solutions there is no visible precipitate. This is due to the small size silica particles that are negatively charged and thus they do not aggregate. We had to resort to partial solvent evaporation in order to isolate silica particles in solid form. Their morphology is shown in row 1. Particles appear dense and the common spherical shape is absent.

In the presence of PCH (rows 2 and 3) the gradual SiO_2 particle growth is obvious. Particles are distorted spheres and their size appears to be ~100 nm after 8 h, growing to ~300–500 nm after 72 h and finally transforming into large aggregates (~2 μm) composed of smaller particles after 4 weeks.

The effect of 20 ppm PEI (a comparable inhibitor to PCH at 40 ppm) on silica particle morphology is similar to that of PCH (see row 4), however the silica aggregates that form are larger in size. This may be due to the high cationic charge of PEI that agglomerates the partially negatively charged silica particles.

Combinations of PCH (40 ppm) and PEI (20 ppm) induce formation of distinctly different silica precipitates (see row 5) than those formed by the separate action of either PCH (rows 2 and 3) or PEI alone (row 4). The silica precipitate collected after 8 h or 72 h appears as a fairly uniform film, composed of ~150–200 nm sized particles. However, upon prolonged polymerization times the precipitate appears to have a porous structure. Profound effects of linear PEI on sodium silicate solutions (pH 9.4) that effect formation of porous silica precipitates have been reported recently [109].

PCH (150 ppm)/CMI (50 ppm) combinations cause formation of visibly more discrete SiO_2 particles after 8 h (see row 6). After 72 h and 4 weeks growth of SiO_2 particles is gradual with no large aggregates forming. However, PCH (150 ppm)/CMI (100 ppm) combinations (see row 7) direct the precipitation of large SiO_2 particles (~2 μm) after 8 h.
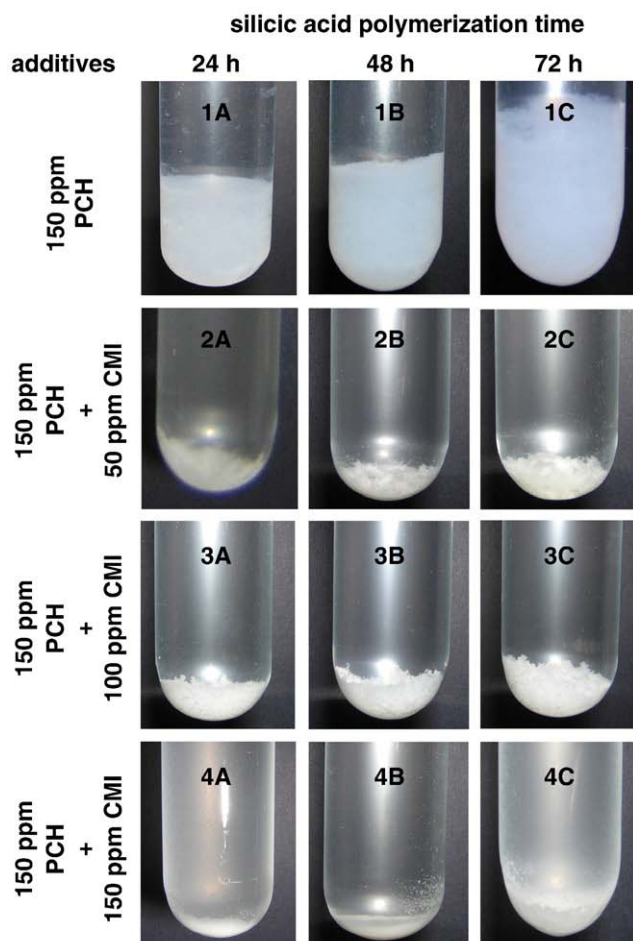
Fig. 12. Visual observations of the effects of PCH/CMI blends on colloidal silica precipitates.
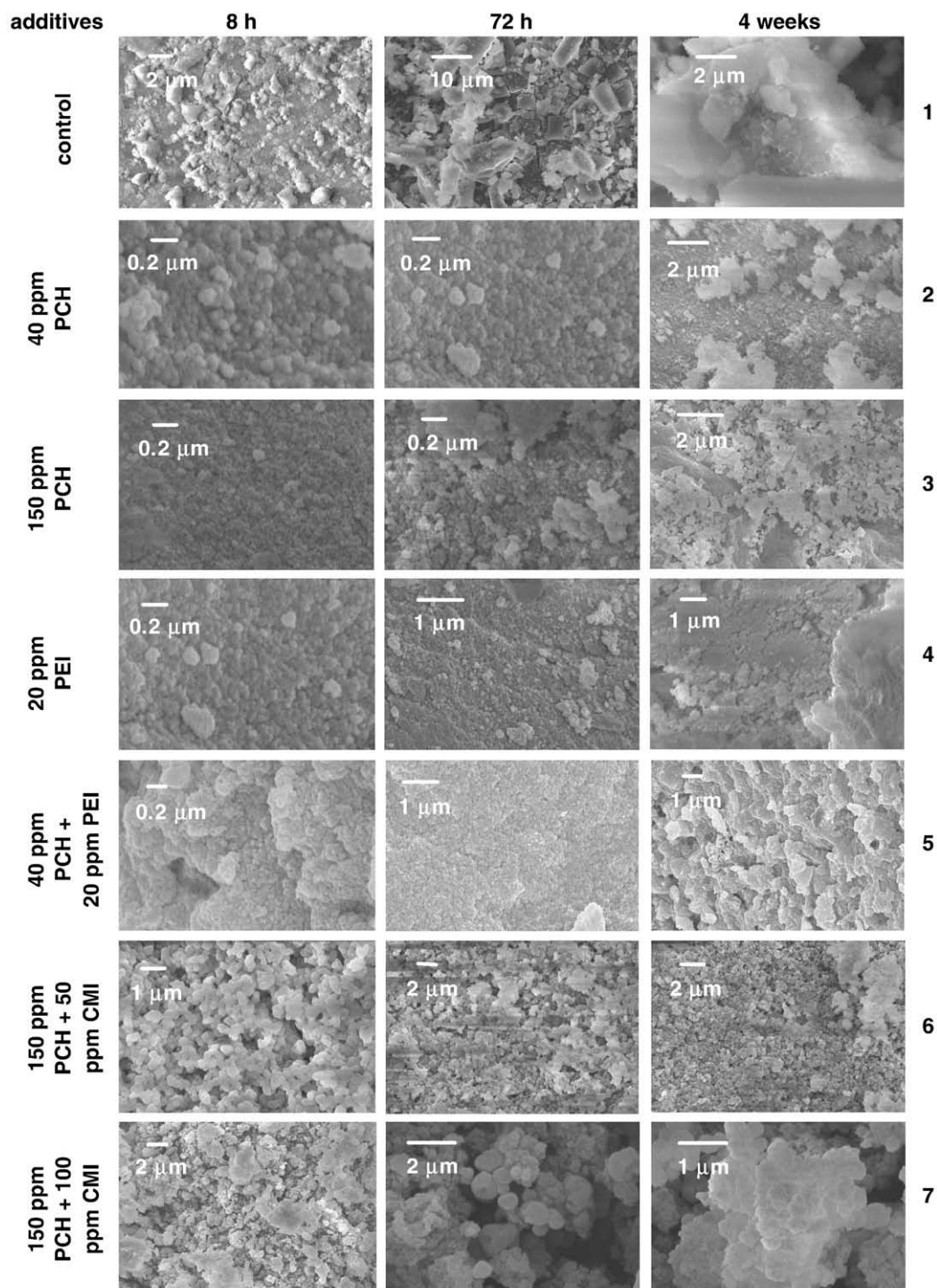
Fig. 13. Effects of PCH, PEI, and PEI/PCH or PCH/CMI combinations on amorphous silica particle morphology. Note the differences in scale. Rows 3, 6, and 7 have been reproduced with permission from Ref.[78] for comparison purposes.

After 72 h particle aggregation continues and also well-shaped spherical particles (~0.5 μm) appear. Finally, upon prolonged particle growth times (4 weeks) flower-shaped structures are formed.

Based on the above results, CMI plays a profound role not only in silicic acid stabilization, but also in SiO_2 particle morphogenesis. Although formation of SiO_2 precipitates is inhibited, their particle size appears larger. This may be related to the slower SiO_2 particle formation that allows more even growth in the presence of PCH/CMI.

5. Discussion

The diatom is an ideal biosystem for investigation of the mechanism of silicon transport, which is an integral part of the biosilicification process [110]. As the environmental concentrations of "dissolved silicon" are rather low (~70 μM), diatoms must have an efficient transport system. Silicon (as orthosilicic acid or silicate) must not only be transported into the cell, but also transported intracellularly into the

SDV where silica morphogenesis occurs. The cells maintain pools of dissolved silicon (in whichever chemical form) in relatively high silicon concentrations. It should be noted that although the intracellular silica pool can be as high as 450 to 700 nM/cell [111], the actual level seems to range from less than 1 mM to about 20 mM (equivalent to a solution of ~1% w/v SiO_2) as recalculated from the silica content and the biovolume for more than 70 species that have been compared for their silica content [112]. Silicon is taken up only during a specific time in the cell cycle (just prior to cell wall synthesis), and the kinetic parameters for silicon transport were found to vary during the uptake period [113]. The above observations point to the necessity of maintaining a relatively high "Si" concentration (above silicic acid "normal" solubility) for a period of time, before its condensation and uptake for the construction of the cell wall. Therefore, the research described herein on enhancement of soluble "Si" levels induced by specifically designed multifunctional biomacromolecules can be from a biomimetic point of view linked to a similar intracellular action in the SDV.

It has been reported that chitosan (CHS, Fig. 1) can catalyze the slow aggregation of colloidal silica nanoparticles in weakly acidic solution even though it did not significantly increase the rate of silica polycondensation [114]. Some of these observations and mechanistic interpretation were met with skepticism [115]. Our approach, although based on utilization of water-soluble silicate as the silica source, is different in many respects: (a) It utilizes a modified chitosan, in which phosphonate groups have been chemically introduced by design. PCH is a polymer possessing both cationic and anionic charge, in contrast to CHS that is purely cationic. (b) The pH of the condensation reaction is 7.00, compared to that of Chang et al. that is substantially lower (pH = 4.0–5.6). (c) The initial silicate

concentration in our experiments is 500 ppm (as SiO_2), corresponding to ~0.00833 M, much lower than that used in chitosan-accelerated experiments (0.04641 M) mentioned above. (d) The focus of our experiments was on delaying silicic acid condensation for an extended period of time, while collecting morphological characterization data on silica particles that formed due to inhibitor imperfection.

An analysis of the above results was sought in an effort to correlate molecular structure and inhibitory activity. This approach is presented in detail in Table 1. There are a number of facts and hypotheses taken into account for this: (a) All anionic polyelectrolytes do not exhibit any inhibitory activity at dosages of up to 200 ppm, as verified experimentally. (b) The PCH amine groups (actually in their protonated form at the experimental pH) are involved in inhibition. (c) Each $=NH^+$–group (to which two methylenephosphonate groups are attached) stabilizes one silicate molecule, each $-NH_2^+$–group (to which one methylenephosphonate groups is attached) stabilizes two silicate molecules, and each $-NH_3^+$ (on the D-glucosamine groups) stabilizes three silicate molecules via, presumably, a combination of electrostatic and hydrogen bonding interactions. This theoretical estimation leads to 1884 silicate molecules stabilized per one polymer chain of PCH. (d) the amide groups (Me–C(O)–NH-ring) do not contribute to inhibitory activity.

Careful examination of the data presented in Table 1 shows that PCH alone (in the absence additional polymeric additives) is incapable of stabilizing the "stoichiometrically" predicted amount of silicate when present at levels up to 40 ppm. It should be noted that when "inhibitor efficiency" is 1, then the amount of silicate stabilized in soluble form is the same as that predicted by the appropriate calculations. It is obvious that for maintaining high "Si" levels soluble

Table 1
Silicic acid stabilization data and analysis by PCH, PEI and PCH/PEI and PCH/CMI combinations.

Polymeric additive (s)	Polymer molar concentration (M)	Polymer molar ratio (PCH/PEI or PCH/CMI)	Soluble silicic acid stabilization (ppm)[a]	Soluble silicic acid (M)	Soluble silicic acid/ PCH molar ratio	Estimated silicic acid/ polymer molar ratio[b]	Inhibitor efficiency[g]
PCH (10 ppm)	3.94×10^{-8}	–	1	1.92×10^{-5}	487	1884[c]	0.26
PCH (20 ppm)	7.88×10^{-8}	–	5	9.60×10^{-5}	1218	1884[c]	0.65
PCH (40 ppm)	1.58×10^{-7}	–	12	2.31×10^{-4}	1462	1884[c]	0.78
PCH (60 ppm)	2.36×10^{-7}	–	51	9.81×10^{-4}	4157	1884[c]	2.21
PCH (100 ppm)	3.94×10^{-7}	–	78	1.50×10^{-3}	3807	1884[c]	2.02
PCH (150 ppm)	4.73×10^{-7}	–	121	2.33×10^{-3}	4926	1884[c]	2.61
PCH (200 ppm)	7.88×10^{-7}	–	122	2.35×10^{-3}	2982	1884[c]	1.58
PEI (10 ppm)	1.43×10^{-7}	–	82	1.58×10^{-3}	11049	1667[d]	6.63
PEI (20 ppm)	2.86×10^{-7}	–	31	5.96×10^{-4}	2084	1667[d]	1.25
PEI (40 ppm)	5.72×10^{-7}	–	23	4.42×10^{-4}	773	1667[d]	0.46
PEI (60 ppm)	8.58×10^{-7}	–	0	0	0	1667[d]	0
PEI (80 ppm)	1.14×10^{-6}	–	0	0	0	1667[d]	0
CMI (50 ppm)	2.00×10^{-5}	–	0	0	0	–[e]	0
CMI (100 ppm)	4.00×10^{-5}	–	0	0	0	–[e]	0
CMI (150 ppm)	6.00×10^{-5}	–	0	0	0	–[e]	0
CMI (200 ppm)	8.00×10^{-5}	–	0	0	0	–[e]	0
PCH (20 ppm) + PEI (20 ppm)	$7.88 \times 10^{-8} + 2.86 \times 10^{-7}$	0.28	116	2.23×10^{-3}	28299	3551[f]	7.97
PCH (40 ppm) + PEI (20 ppm)	$1.58 \times 10^{-7} + 2.86 \times 10^{-7}$	0.55	79	1.52×10^{-3}	9620	3551[f]	2.71
PCH (60 ppm) + PEI (20 ppm)	$2.36 \times 10^{-7} + 2.86 \times 10^{-7}$	0.83	73	1.40×10^{-3}	5932	3551[f]	1.67
PCH (150 ppm) + CMI (100 ppm)	$4.73 \times 10^{-7} + 4.00 \times 10^{-5}$	0.01	5	9.60×10^{-5}	203	1884	0.11
PCH (150 ppm) + CMI (150 ppm)	$4.73 \times 10^{-7} + 6.00 \times 10^{-5}$	0.008	1	1.92×10^{-5}	41	1884	0.02
PCH (150 ppm) + CMI (200 ppm)	$4.73 \times 10^{-7} + 8.00 \times 10^{-5}$	0.006	44	8.46×10^{-4}	1910	1884	1.01

[a] These data indicate measured soluble silicic acid (in ppm) at 24 h after subtraction of soluble silicic acid without additives (control).

[b] The estimation of the predicted silicate/polymer molecular ratio was based on the hypothesis that $a \equiv NH^+$ group stabilizes one silicate molecule, $a = NH_2^+$ stabilizes two silicate molecules and a $-NH_3^+$ group stabilizes three silicate molecules.

[c] Polymer = PCH in this case.

[d] Polymer = PEI in this case.

[e] Polymer = CMI in this case. CMI does not possess amine groups.

[f] The total number of N–H groups calculated (coming from both PCH and PEI) is 1884 (from PCH) + 1667 (from PEI) = 3551.

[g] Defined as the number of silicate molecules stabilized as found experimentally divided by the estimated silicate molecules stabilized per chain of polymer. Inhibitor efficiency of 1 means that the predicted ("stoichiometric") amount of silicate remains soluble. Naturally, the higher this number is, the more efficient the inhibitor is. When inhibitor efficiency is >1, then the polymer acts as silicic acid condensation inhibitor. When inhibitor efficiency is <1, then the polymer acts as silicic acid condensation catalyst.

beyond silicic acid supersaturation, "inhibitor efficiency" should be >1. PCH at 60 ppm level stabilizes 2.21 times more silicates than what is predicted by the aforementioned analysis. The highest "inhibitor efficiency" is achieved at 150 ppm PCH, 2.61. PEI at only 10 ppm levels displays inhibitor efficiency of 6.63, but that drops substantially as PEI dosage is increased (0.46 at 80 ppm PEI). Combinations of PCH and PEI (20 ppm each) appear to stabilize almost 8 times more silicate than calculated. Finally, PCH and CMI combinations exhibit very low efficiencies. Only at higher levels of PCH (150 ppm) and CMI (200 ppm) efficiency is ~1.

Inhibition of silica growth is not entirely understood. It should be emphasized that silicic acid polymerization inhibition and colloidal silica stabilization are two completely different approaches. The latter aims at maintaining small silica colloids dispersed (in suspension) and at avoidance of deposition. In contrast, the former delays (ideally ceases) silicic acid polymerization, thus maintaining silicate in its soluble forms. Colloidal silica ideally does not form in that case. This approach is sought in this research. The inhibitor "disrupts" condensation polymerization of silicic acid by interfering with nucleophilic attack of neighboring silicate ions (an S_N2-like mechanism).

PCH associates with silicic acid molecules and silicate ions or small silica oligomers, thus preventing further growth. As mentioned above, the silica supersaturations achieved in the presence of PCH (Table 1) support the conclusion that silicic acid stabilization is not a stoichiometric phenomenon [116–120].

This is further supported by the effect of PEI, which is purely cationic [102]. A reasonable hypothesis that stabilized larger (oligo) silicates must be present either within loops formed by PCH (or PEI) chain folding or at the interface of neighboring polymer chains, can be put forth. Unfortunately, the silicomolybdate test cannot distinguish between various forms of silicates. CMI apparently cannot function similarly, because the negative charge from the carboxylate groups is dominant. It is well established that anionic small molecules and polymers do not affect silicic acid polymerization.

5.1. Biopolymer entrapment into the silica matrix

Several literature reports confirm that polymers bearing cationic charge are entrapped into the colloidal silica matrix, either in vivo (the presence of proteins is well documented) [15–17,19,21] or in vitro. For example, poly(allylamine hydrochloride)-accelerated TMOS hydrolysis produced well-defined silica structures at neutral pH and ambient conditions. The polymer was found to be incorporated into the silica particles [36]. Similarly, chitosan-induced silica formation leads to polymer entrapment in silica, as confirmed by FT-IR spectroscopy [114]. Amine-terminated PAMAM dendrimers were identified by FT-IR spectro-

scopy and elemental analysis in silica precipitates [71–78,90,104,121]. Polylysine was found to be incorporated to silica platelets [122].

We have acquired FT-IR spectra of all silica precipitates in the presence of these polymers. The results are shown in Fig. 14.

FT-IR of precipitates that result from solutions containing PCH show that PCH is entrapped into the silica amorphous matrix. This is supported by examining two spectral regions. First, the main band of amorphous silica at ~1100 cm^{-1} is assigned to the Si–O vibration. The PCH-containing silica precipitates show this main band, but with a fine structure. This is a result of a superposition of the Si–O band and the wide band from PCH assigned to the P=O and P–O vibrations, also centered around 1100 cm^{-1}. The region 1300–1700 cm^{-1} is more revealing. Two bands at ~1650 and 1580 cm^{-1} from the ν(C=O)as vibrations of the PCH amide functionality (spectrum 2) were also located in the spectrum of the silica–PCH composite, see spectrum 3. In PCH/CMI/silica composite precipitates, the characteristic asymmetric ν(C=O)$_{asym}$ (1598 cm^{-1}) and symmetric ν(C–O)$_{sym}$ (1400 cm^{-1}) vibrations from CMI carboxylate moieties (and possibly from the PCH amide group) are evident (see spectrum 7). These match very well with those of pure CMI (spectrum 6). Silica precipitates formed in the presence of PEI show bands ~1630 cm^{-1} and ~1400 cm^{-1} (spectrum 5) that are also present in pure PEI (spectrum 4).

PCH entrapment in the colloidal silica matrix can only be explained by invoking the ability of the polymer to act as a bridge between SiO$_2$ particles. Its high molecular weight allows for its interaction with a large number of silica particles through the –NH$_3^+$ moieties and possibly through the –NH^{+}···(phosphonate)$_2$ and/or –NH$_2^{+}$··· (phosphonate) groups. These interactions are possibly a combination of electrostatic attraction and hydrogen bonding with the partially deprotonated silanol surface groups of the silica particles. Possible hydrogen bonding between phosphonate and silanol groups cannot be excluded, but these are expected to be minor. One can visualize these interactions as shown schematically in Fig. 15.

Several studies have been carried out on the acid base behavior and negative charge on silica particles [123–129]. It was calculated that the silanol groups on the silica surface are ~4.6 Si–OH/nm^2. The isoelectric point of silica was found to be ~2. This means that after that value of solution pH silanol groups start losing protons to become negatively charged –Si–O$^-$ moieties. Iler reported that it is only at pH~7 substantial number of –Si–O$^-$ moieties accumulate [130]. In fact, the density of –Si–O$^-$ groups was calculated at pH 9 and it was found to be 0.63 –Si–O$^-$/nm^2. At this point the exact charge density of –Si–O$^-$ groups at pH 7 (where all our experiments were carried out) is not known, but it is certainly lower than 0.63 –Si–O$^-$/nm^2. Therefore, there seems to be sufficient negative charge on the silica particles (formed due to inability of PCH and its combination with either PEI or CMI to inhibit all 500 ppm initial silicic acid) to cause
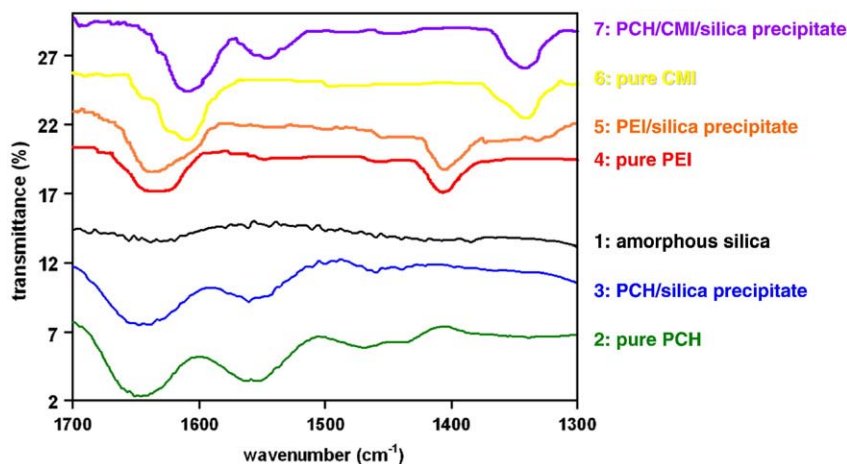

Fig. 14. PCH and PCH/CMI polymer entrapment within the colloidal silica matrix, as demonstrated by FT-IR spectroscopy.
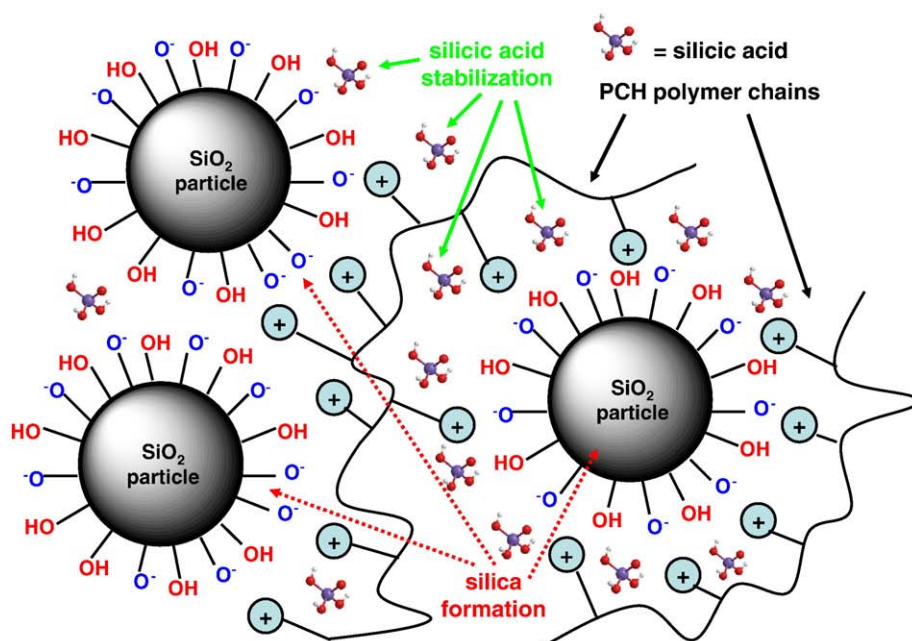
Fig. 15. Schematic representation of colloidal silica–PCH assemblies.

association with positively charged groups of PCH (and PEI). Formation of silica inhibitor assemblies due to electrostatic attraction is experimentally supported by our microscopy studies and FT-IR experiments. We have also performed elemental analyses (CHN) on silica inhibitor precipitates. All three elements were present (results not shown here).

5.2. Structure/function relationships

It is by now well-established that biomacromolecules have to contain positively charged moieties for silicic acid condensation activity. Due to their complexity, however, they contain a plethora of other (negatively charged or neutral) chemical groups, whose involvement in the condensation reaction is poorly understood. There has been a flurry of research efforts to delineate the exact role of these groups in the biosilicification process. Some comments are warranted.

An important study by Patwardhan et al. demonstrated that the handedness of the helicity of polylysine does not affect the formation of hexagonal silica [122]. In addition, formation of polylysine helices is a prerequisite to the hexagonal silica synthesis. Furthermore, when polylysine helices were converted to β-sheet structure, only silica particles were obtained, thus suggesting that the adoption of a helical conformation by polylysine is required for the formation of hexagonally organized silica.

Perry et al. have systematically studied the effect of hydroxyl-containing molecules (such as diols) on silica formation [131]. The results demonstrate that in aqueous systems, the effect of hydroxyl-containing additives is negligible, although as the molar ratio of the Si/OH groups decreases, the effect of these molecules becomes more apparent. It should be noted that the alkanediol concentrations were very high (15–150 mM).

Perry et al. also studied the role of individual and oligomeric amino acids in silicification experiments in vitro [132]. It was found that individual amino acids variously reduced or accelerated the early kinetics of silicate condensation and aggregation and produced silica particles with surface areas which varied according to the isoelectric point of the amino acid. Introduction of polylysine produced a slightly increased enhancement of the early kinetics but dramatically increased aggregation rates as silica condensation progressed, suggesting that aggregation may be a major influence on biosilica formation.

Under chemical influences, overall morphologies were observed to shift from a characteristic network of sphere-like silica particles to a sheetlike structure in the presence of –OH groups from additives and to sharp-edged, platelike structures in the presence of larger polycationic peptide matrixes [133]. Under physical influences, using externally applied force fields, overall silica morphologies were observed to transition from sphere-like to fiber-like and dendrite-like structures. The addition of alcohols and carbohydrates to the standard hydrostatic solutions altered the size of the spherical silica particles normally obtained from in vitro polycationic peptide-mediated biosilicification without additives.

Poly-L-lysine (PLL) promotes the precipitation of silica from a silicic acid solution within minutes [134]. The molecular weight of PLL was found to affect the morphology of the resulting silica precipitate. Larger–molecular weight PLL produced hexagonal silica platelets, whereas spherical silica particles were obtained using low-molecular weight PLL.

Planar immobilized PLL and a functional analogue, propylamine, are effective in promoting the synthesis of silica from a silicic acid precursor under neutral conditions. The size of silica particles is ~30 nm across, that eventually fuse to form an interconnected coating [135].

A range of quaternized tertiary amine methacrylate-based homo-polymers and copolymers were utilized as mimics of the biopolymers implicated in biosilica formation [136]. They were evaluated for their ability to catalyze and direct the structure of silica formed by condensation of silicic acid in aqueous solution and at neutral pH. Homo- and co-polymers of differing degrees of quaternization were studied. All polymers acted as catalysts for the condensation reaction, but at different rates according to their architecture and degree of quaternization. Some crystallites were present in the hybrids and differences in crystal structure were observed in the calcined silicas, depending on the structure of the polymer, indicating that the polymers exert a structure-directing effect during initial silica formation. The work provides some new insights into structural factors affecting silica growth catalyzed by synthetic cationic polymers.

TMOS hydrolytic condensation in the presence of fibrous linear PEI aggregates and monovalent, divalent and trivalent metal ions was studied in order to examine if they can serve as templates for silica deposition [137]. It was found that silicification proceeds site-selectively on the surface of the aggregates, resulting in silica fibers with axial PEI filaments. In conclusion, the linear PEI aggregates regulated by metal
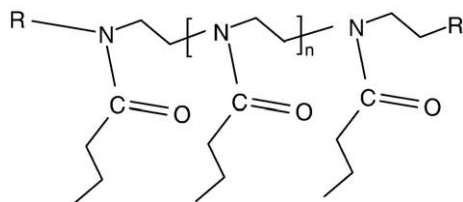
Fig. 16. Schematic structure of polyethyloxazoline polymers backbone.

cations are very effective organic reactors for the synthesis of silica nanocomposites with special dimensions and morphology. Related to that, multiply shaped silica structures (flower-, plate-, bundle-, leaf-, sphere-line) were mediated by aggregates of linear polyethyleneimine [138].

Amorphous silica materials have been prepared by the neutral templating route using amine-terminated dendrimeric templates, while the Si source was TEOS in EtOH/water mixtures. Note the high template concentration in the reaction medium, 1.0 TEOS:0.26 template:9.09 EtOH:50.8 H_2O [139].

Fabrication of lotus-leaf-like nanoporous silica flakes with controlled thickness was achieved by the action of 1-hexadecylamine on TEOS. The amine:TEOS molar ratio was high, 5:24 [140]. Biomimetic micropatterning of silica by surface-initiated polymerization of 2-(dimethylamino)ethyl methacrylate (DMAEMA) with TMOS was observed [141].

Our group has demonstrated that neutral polymers can control silicic acid polymerization. A notable example is polyethyloxazoline, Fig. 16 [142].

Polyethyloxazoline contains amide repeating units, but no N basic moieties. This notwithstanding, it can maintain up to 345 ppm soluble silicic acid in the first 8 h and a bit more than 300 ppm after 24 h. Notably, silicic acid polymerization control seems to be essentially independent of polyethyloxazoline polymer molecular weight. It is worth-noting that PCH also contains amide functionalities, whose specific role cannot be accurately determined at this point.

Recently Perry et al. have used poly(1-vinylimidazole) mass fractions to inhibit silicic acid condensation [143,144]. The "Si" source was sodium silicate. It was reported that very high concentrations of poly(1-vinylimidazole) (5.3 mM) can stabilize ~5 mM silicic acid (or ~ 300 ppm as SiO_2) at pH 7. Based on our results, PCH at much lower concentration, 5.91×10^{-4} mM (150 ppm), can stabilize ~5 mM silicic acid (or ~300 ppm as SiO_2) at pH 7. Direct comparison between the inhibitory activity of these polymers is not possible, due to lack of data on the time dependence of silicic acid stabilization by poly(1-vinylimidazole).

There is rich information in the biosilicification-related literature on additive-induced silica morphogenesis. Additives can be either "small molecules" or polymers. Taking into account these data along with the various structural features responsible for silica precipitation, some useful observations can be noted: (a) The cationic charge (mainly located on protonated amine groups) is necessary. (b) Cationic charge density and the rate of silica formation seem to be directly proportional. (c) Neutral moieties (such as –OH) seem to have negligible effects on silicic acid condensation. (d) Anionic groups seem to play a yet unidentified role in biosilicification. (e) Molecular weight also plays an accelerating role in silica formation. (f) Various silica structures have been obtained by use of biopolymers with different structural features, but a clear structure/function relationship cannot be derived.

Interestingly, most published studies concentrate on the effect of various additives on biosilica morphology. To our knowledge, our work during the last 5 years is the only example (together with recent work by Perry et al. [143,144]) in the literature that focuses on the stabilizing effect of chemical additives on silicic acid. Based on this and previous papers from our laboratory, some facts can be drawn: (a) A certain degree of cationic charge seems to be necessary to achieve high soluble "Si" levels. (b) Partial neutralization of this cationic charge either intramolecularly (by external addition of an anionic polymer) or intramolecularly (by use of zwitterionic additives) usually results in reduction of soluble "Si" levels. (c) The effect of the cationic charge seems to be independent of its nature. In other words, an effective inhibitor may have either protonated amine groups ($-NH_3^+$) or quaternary ammonium groups ($-NR_3^+$). A notable example is the polymer PAMALAM (a copolymer of polyacrylamide and diallyldimethylammonium chloride) [77,145]. Apparently, further structure/function relationships are needed to draw definitive conclusions regarding the structural (and other) features that an effective silica inhibitor must possess.

6. Conclusions/outlook

The purpose of this work is to identify and exploit novel polymeric structures that are able not only to direct silica morphogenesis, but also to maintain high silicic acid concentrations for an extended period of time before silica deposition occurs. This is directly linked to silicon cargo transport to and within the cell, during which relatively high "Si" concentrations must be maintained for a period of time. It should be noted that there is also an intense interest in the water treatment industry, where chemical technologies for effective silica scale growth in process waters are still an unsolved problem.

The principle findings are summarized as follows: (1) PCH can maintain soluble silicic acid levels beyond the calculated level at >60 ppm dosages. (2) PEI maintains higher silicic acid levels compared to PCH, at lower (10 ppm) levels. (3) PCH/PEI combinations are effective inhibitors of silicic acid condensation at rather low levels (20 ppm each). (4) CMI appears to have detrimental effects on the inhibitory activity of PCH. (5) PCH, with ammonium/phosphonate-containing structural features also acts as a silica aggregator forming SiO_2–PCH composites with subsequent loss of inhibitor efficiency over time due to inhibitor entrapment within the amorphous 3D silica matrix. These composites could be envisioned as colloidal silica particles "glued" together with PCH.

Dependence of inhibition ability on particular structural features of the inhibitor molecule is of great importance. Structure/activity relationships may help in the rational design of inhibitors with precise structures and topologies that may show, ideally, predictable inhibition performance. Inhibition of silica growth most probably occurs at the early stages of silicic acid polymerization. Unfortunately, there is little information available at the molecular level on the silicate oligomers formed. Such data would be of great importance, because they would greatly facilitate inhibitor design and improvement.

The presence of polyamines on the silaffins not only provides a possible template for nucleation, but might also control the silica colloid size within the SDV [146]. The globular silica particles observed to constitute diatom silica may reflect the chain lengths of the polyamines that are used to direct silica deposition. Other molecules may have an inhibitory effect on silicification, even in the presence of the nucleating molecules. It will be important to determine how the activities of one group of molecules modulate the activities of another. The answer to this question will be of value in developing the means to manipulate nanofabrication in materials science.

The entire biological process for biosilica formation, from initial "Si" uptake, to its (extracellular or intracellular) transport to the final silica synthesis, is obviously an intricately complicated array of diverse pathways. One should also keep in mind the significant findings of Kinrade et al. who discovered by ^{29}Si NMR spectroscopy that carbohydrate-like molecules can covalently interact with silicate to form five, and six-coordinated stable silicon complexes [147,148]. His observations shed new light to the issue of silicon transport and, perhaps, intracellular stabilization, but add one more variable to the biosilicification process: that polysaccharide-like polymers (and "small" molecules [149]), perhaps originating from the diatom cell wall can affect "Si" transport and/or condensation.

Perry et al. have extracted protein-containing biomolecules from intrasilica locations in the branches of *Equisetum telmateia* and used them in the study of silica precipitation at circumneutral pH [150]. The biopolymer extract used in this study was released by solubilization of the siliceous phase with buffered solutions of HF following treatment of plant materials with a mixture of concentrated nitric and sulfuric acids. The amino acid composition of this extract was rich in serine, glutamine/glutamic acid and glycine. A significant finding was that this extract had associated with it a carbohydrate component enriched in glucose and xylose.

Finally, Sumper et al. recently reported the isolation and characterization of peptides from diatom *Thalassiosira pseudonana* silica that are polyanionic and rich in aspartate/glutamate and serine phosphate [151]. The term "silacidins" was coined for these peptides. It was reported that silicidins serve as biologically relevant agents that guide the assembly of polyamines, which, in turn, catalyze the condensation of silicic acid for biosilica production. This polyamines/silacidins dual supramolecular system undoubtedly proves the importance of biopolymer assembly in biosilicification. In parallel, the complexity of this system presents a first class opportunity for biomimetic, *in vitro* approaches and strategies to silica synthesis.

Silicon, the basis of semiconductors and many advanced materials, is an essential element for higher plants and animals, yet its biology is incompletely understood. This, however, presents a unique opportunity for interdisciplinary research to go forward and reveal yet additional unique and exciting secrets of biosilicification. Many invertebrates produce exquisitely controlled silica structures with a nanoscale precision exceeding present human ability. Biotechnology is starting to reveal the proteins, genes and molecular mechanisms that control this synthesis in marine organisms that produce large amounts of silica, as well as diatom silicon transporters [152–154].

Valuable information from biology must be combined with findings from classical sol-gel science [155,156] in an integrative way. Uncovering the mechanisms governing biosilicification offers the prospect of developing environmentally benign routes [157,158] to synthesize new silicon-based materials and to resolve the biological use of silicon in higher organisms.

Acknowledgements

References

[1] Pohnert G. Angew Chem Int Ed 2002;41:3167–9.
[2] Coradin T, Lopez PJ, Gautier C, Livage J. C R Palevol 2004;3:443–52.
[3] Schröder HC, Wang X, Tremel W, Ushijima H, Müller WEG. Nat Prod Rep 2008;25:455–74.
[4] Tréguer P, Nelson DM, Van Bennekom AJ, DeMaster DJ, Leynaert A, Quéguiner B. Science 1995;268:375–9.
[5] Sun Q, Vrieling EG, van Santen RA, Sommerdijk NAJM. Curr Opin Solid State Mater Sci 2004;8:111–20.
[6] Maldonado M, Carmona MC, Velasquez Z, Puig A, Cruzado A, Lopez A, et al. Limnol Oceanogr 2005;50:799–809.
[7] Fairhead M, Johnson KA, Kowatz T, McMahon SA, Carter LG, Oke M, et al. Chem Comm 2008:1765–7.
[8] Schwartz K. Proc Natl Acad Sci 1973;70:1608–12.
[9] Ehrlich H, Krautter M, Hanke T, Simon P, Knieb C, Heinemann S, et al. J Exp Zool (Mol Dev Evol) 2007;308B:473–83.
[10] Ehrlich H, Worch H. In: Custodio MR, Lobo-Hajdu G, Hajdu E, Muricy G, editors. Porifera Research: Biodiversity, Innovation & Sustainability; 2007. p. 217–23.
[11] Ehrlich H, Janussen D, Simon P, Heinemann S, Bazhenov VV, Shapkin NP, et al. J Nanomater 2008 [Article ID 670235].
[12] Ehrlich H, Ereskovsky A, Drozdov A, Krylova D, Hanke T, Meissner H, et al. Russ J Mar Biol 2006;32:186–93.
[13] Ehrlich H, Worch H. In: Bäurlein E, editor. Handbook of Biomineralization. The Biology of Biominerals Structure FormationWeinheim: Wiley VCH; 2007. p. 23–41. Chapter 2.
[14] Ehrlich H, Heinemann S, Heinemann C, Simon P, Bazhenov V, Shapkin N, et al. J Nanomater 2008 [Article ID 623838].
[15] Coffman EA, Melechko AV, Allison DP, Simpson ML, Doktycz MJ. Langmuir 2004;20:8431–6.
[16] Ogasawara W, Shenton W, Davis SA, Mann S. Chem Mater 2000;12:2835–7.
[17] Poulsen N, Sumper M, Kröger N. Proc Natl Acad Sci 2003;100:12075–80.
[18] Zhou Y, Shimizu K, Cha JN, Stucky GD, Morse DE. Angew Chem Int Ed 1999;38:779–82.
[19] Kroger N, Lorenz S, Brunner E, Sumper M. Science 2002;298:584–6.
[20] Cha JN, Shimizu K, Zhou Y, Christiansen SC, Chemelka BF, Stucky GD, et al. Proc Natl Acad Sci 1999;96:361–5.
[21] Morse DE. Trends Biotechnol 1999;17:230–2.
[22] Kroger N, Deutzmann R, Sumper M. Science 1999;286:1129–32.
[23] Kroger N, Deutzmann R, Sumper M. J Biol Chem 2001;276:26066–70.
[24] Wenzl S, Deutzmann R, Hett R, Hochmuth E, Sumper M. Angew Chem Int Ed 2004;44:5933–6.
[25] Vrieling EG, Beelen TPM, Gieskes WWC. J Phycol 1999;35:548–59.
[26] Vrieling EG, Beelen TPM, van Santen RA, Gieskes WWC. Angew Chem Int Ed 2002;41:1543–6.
[27] Hazelar S, van der Strate HJ, Gieskes WWC, Vrieling EG. J Phycol 2005;41:354–8.
[28] Gordon R, Drum RW. Int Rev Cytol 1994;150:243–372.
[29] Sumper M. Science 2002;295:2430–3.
[30] Knecht MR, Wright DW. Chem Comm 2003;24:3038–9.
[31] Kroger N, Deutzmann R, Bergsdorf C, Sumper M. Proc Natl Acad Sci 2000;97: 14133–8.
[32] Coradin T, Livage J. Acc Chem Res 2007;40:819–26.
[33] Tomczak MM, Glawe DD, Drummy LF, Lawrence CG, Stone MO, Perry CC, et al. J Am Chem Soc 2005;127:12577–82.
[34] Coradin T, Lopez PJ. ChemBioChem 2003;4:251–9.
[35] Coradin T, Durupthy O, Livage J. Langmuir 2002;18:2331–6.
[36] Patwardhan SV, Clarson SJ. J Inorg Organomet Polym 2003;13:193–203.
[37] Patwardhan SV, Clarson SJ. J Inorg Organomet Polym 2003;13:49–53.
[38] Patwardhan SV, Mukherjee N, Clarson SJ. Silicon Chem 2002;1:47–55.
[39] Patwardhan SV, Mukherjee N, Clarson SJ. J Inorg Organomet Polym 2002;11:193–8.
[40] Patwardhan SV, Mukherjee N, Clarson SJ. J Inorg Organomet Polym 2002;11:117–21.
[41] Patwardhan SV, Clarson SJ. Silicon Chem 2002;1:207–14.
[42] Robinson DB, Rognlien JL, Bauer CA, Simmons BA. J Mater Chem 2007;17: 2113–9.
[43] Menzel H, Horstmann S, Behrens P, Bärnreuther P, Krueger I, Jahns M. Chem Commun 2003:2994.
[44] Jones SM. J Non-Cryst Solids 2001;291:206–10.
[45] Annenkov VV, Patwardhan SV, Belton D, Danilovtseva EN, Perry CC. Chem Commun 2006:1521–3.
[46] Tanev PT, Liang Y, Pinnavaia TJ. J Am Chem Soc 1997;119:8616–24.
[47] Adeogun MJ, Hay JN. Polymer Int 1996;41:123–34.
[48] Hentze H-P, Raghavan SR, McKelvey CA, Kaler EW. Langmuir 2003;19:1069–74.
[49] Martin-Jezequel V, Hildebrand M, Brzezinski MA. J Phycol 2000;36:821–40.
[50] Schmid A-MM, Schulze D. Protoplasma 1979;100:267–88.
[51] Hildebrand M, Wetherbee R. Prog Mol Subcell Biol 2003;33:11–57.
[52] Davis AK, Hildebrand M. In: Sigel A, Sigel H, Sigel RKO, editors. Biomineralization: From Nature to Application (Metal Ions in Life Sciences). Chechester: Wiley; 2008.
[53] Bhattacharyya P, Volcani BE. Biochem Biophys Res Commun 1983;114:365–72.
[54] Five Silicon Transporter Genes (SITs) have been discovered (see Hildebrand, M., Dahlin, K., Volcani, B.E. Mol. Gen. Genet. 1998, 260, 480–486). Their expression is induced simultaneously, just prior to the period of maximum silicon incorporation into the cell wall, and levels decrease by the end of that period. This is consistent with a single mechanism of silicon uptake control *i.e.* the induction and repression of transport activity at specific times in the cell cycle.
[55] Simpson TL, Volcani BE, editors. Silicon and Siliceous Structures in Biological Systems. New York: Springer-Verlag; 1981.
[56] Kolb VM, Philip AI, Perry RS. In: Hoover RB, Levin GV, Rozanov AY, editors. Instruments, Methods, and Missions for Astrobiology VIII. SPIE; 2004. p. 116–25.
[57] Icopini GA, Brantley SL, Heany PJ. Geochim Cosmochim Acta 2005;69:293–303.
[58] Erdogdu G, Hasirci V. Environ Res A 1998;78:38–42.
[59] Carlisle EM. In: Evered D, O'Connor M, editors. Silicon Biochemistry, Ciba Symposium 121. Chichester, UK: Wiley & Sons; 1986. p. 123–39.
[60] Gillette-Guyonnet S, Andrieu S, Nourhashemi F, de La Guéronnière V, Grandjean H, Vellas B. Am J Clin Nutr 2005;81:897–902.
[61] Jugdaohsingh R, Reffitt DM, Oldham C, Day JP, Fifield LK, Thompson RPH, et al. Am J Clin Nutr 2000;71:944–9.
[62] Bishop M, Bott SG, Barron AR. Chem Mater 2003;15:3074–88.
[63] Bourg S, Broudic J-C, Conocar O, Moreau JJE, Meyer D, Wong Chi Man M. Chem Mater 2001;13:491–9.
[64] Dubin L. In: Sikes CS, Wheeler AP, editors. Surface Reactive Peptides and Polymers: Discovery and Commercialization. Washington DC: American Chemical Society; 1991. p. 355–79.
[65] Iler RK. The Chemistry of Silica. New York: Wiley-Interscience; 1979.
[66] Lindberg R, Sundholm G, Pettersen B, Sjöblom J, Friberg SE. Colloids Surf A Physicochem Eng Asp 1997;123–124:549–60.
[67] Sjöberg S. J Non-Cryst Solids 1996;196:51.
[68] Silica deposits can be cleaned mechanically by "sandblasting", or chemically with $NH_4F \cdot HF$, a process that is not free from hazards: Frenier, W. Technology for Chemical Cleaning of Industrial Equipment, NACE: Houston; 2000.
[69] We have recently reported on environmentally friendly chemical cleaning approaches for silica dissolution: Demadis, K.D., Mavredaki, E. Environ. Chem. Lett. 2005, 3, 127–131.
[70] Demadis KD. Chem Process 2003;66(5):29–32.

[71] Demadis KD, Neofotistou E. Mater Perform 2004;43(4):38–42.
[72] Neofotistou E, Demadis KD. Colloids Surf A Physicochem Eng Asp 2004;242: 213–6.
[73] Demadis KD. J Chem Technol Biotechnol 2005;80:630–40.
[74] Demadis KD, Neofotistou E, Mavredaki E, Tsiknakis M, Sarigiannidou EM, Katarachia SD. Desalination 2005;179:281–95.
[75] Demadis KD. In: Delgado Daniel J, Moreno Pablo, editors. Desalination Research Progress. New York: Nova Science Publishers, Inc.; 2008. p. 249–59. Chapter 6.
[76] Mavredaki E, Neofotistou E, Demadis KD. Ind Eng Chem Res 2005;44:7019–26.
[77] Demadis KD, Stathoulopoulou A. Ind Eng Chem Res 2006;45:4436–40.
[78] Demadis KD, Ketsetzi A, Pachis K, Ramos VM. Biomacromolecules 2008;9: 3288–93.
[79] Ravi Kumar MNV. React Funct Polym 2000;46:1–27.
[80] Yi H, Wu L-Q, Bentley WE, Ghodssi R, Rubloff GW, Culver JN, et al. Biomacromolecules 2005;6:2881–94.
[81] Schwarzenbach G, Ackermann H, Ruckstuhl P. Helv Chim Acta 1949;32:1175–86.
[82] Hecky RE, Mopper K, Kilham P, Degens ET. Mar Biol 1973;19:323–31.
[83] Tacke R. Angew Chem Int Ed 1999;38:3015–8.
[84] Heras A, Rodriguez NM, Ramos VM, Agullo E. Carbohydr Polym 2001;44:1–8.
[85] Ramos VM, Rodriguez NM, Rodriguez MS, Heras A, Agullo E. Carbohydr Polym 2003;51:425–9.
[86] Ramos VM, Rodriguez NM, Diaz MF, Rodriguez MS, Heras A, Agullo E. Carbohydr Polym 2003;52:39–46.
[87] Verraest DL, Peters JA, Batelaan JG, van Bekkum H. Carbohydr Res 1995;271: 101–12.
[88] Kari G, Rodeck U, Dicker AP. Clin Pharmacol Ther 2007;82:70–80.
[89] Dautremepuits C, Paris-Palacios S, Betoulle S, Vernet G. Comp Biochem Physiol C Toxicol Pharmacol 2004;137:325–33.
[90] Demadis KD, Neofotistou E. Desalination 2004;167:257–72.
[91] Coradin T, Eglin D, Livage J. Spectroscopy 2004;18:567–76.
[92] Alexander GB. J Am Chem Soc 1953;75:5655–7.
[93] Truesdale VW, Smith PJ, Smith CJ. Analyst 1979;897–918.
[94] Truesdale VW, Smith CJ. Analyst 1975:797–805.
[95] Truesdale VW, Smith CJ. Analyst 1975:203–12.
[96] Simmons et al. (reference 42) have reported that "small" ammonium-based additives accelerate phosphate-buffered silicate condensation to form colloidal silica at additive and silicate concentrations of 10 mM and 90 mM, respectively. It is obvious that our approach and respective results from our research are not directly comparable.
[97] Coradin T, Livage J. Colloids Surf B Biointerfaces 2001;21:329–36.
[98] Leisner D, Imae T. J Phys Chem B 2004;108:1798–804.
[99] Leisner D, Imae T. J Phys Chem B 2003;107:13158–67.
[100] McKenna BJ, Birkedal H, Bartl MH, Deming TJ, Stucky GD. Angew Chem Int Ed 2004;43:5652–5.
[101] There is a recent relevant report on the biomimetic synthesis of titanium dioxide utilizing the R5 peptide derived from Cylindrotheca fusiformis: Sewell, S.L.; Wright, D.W. Chem Mater 2006, 18, 3108–3113.
[102] The first protonation step occurring at pH around 9.5 corresponds to the protonation of the primary amine groups on the side chains. During the second protonation step at pH around 4.5 every second tertiary amine protonates. The final protonation step, where the remaining tertiary amines protonate, is suspected to occur in a pH range near 0. Koper, G.J.M.; van Duijvenbode, R.C.; Stam, D.D.P.W.; Steuerle, U.; Borkovec, M. Macromolecules 2003, 36, 2500–2507.
[103] Euvrard M, Hadi L, Foissy A. Desalination 2007;205:114–23.
[104] Demadis KD, Neofotistou E. Chem Mater 2007;19:581–7.
[105] Vrieling EG, Sun O, Tian M, Kooyman PJ, Gieskes WWC, van Santen RA, et al. Proc Natl Acad Sci 2007;104:10441–6.
[106] Rothbaum HP, Rohde AG. J Colloid Interface Sci 1979;71:533–59.
[107] Bohlmann EG, Mesmer RE, Berlinksi P. Soc Pet Eng J 1980;20:239–48.
[108] Patwardhan SV, Mukherjee N, Steinitz-Kannan M, Clarson SJ. Chem Comm 2003: 1122–3.
[109] Zhu P-X, Jin R-H. J Mater Chem 2008;18:313–8.
[110] Hildebrand M, Volcani BE, Gassmann W, Schroeder JI. Nature 1997;385:688–9.
[111] Robinson DH, Sullivan CW. Trends Biol Sci 1987;12:151–4.
[112] Conley DJ, Kilham SS, Theriot E. Limnol Oceanogr 1989;34:205–13.
[113] The exact "timing" for the initiation of silicate condensation is not known. However, a set of silaffins isolated from diatom cell walls were shown to generate networks of silica nanospheres within seconds when added to a solution of silicic acid: see Ref. 22. Furthermore, natSil-2 lacks intrinsic silica formation activity but is able to regulate the activities of the previously characterized silica-forming biomolecules natSil-1A and long-chain polyamines. Combining natSil-2 and natSil-1A (or long-chain polyamines) generates an organic matrix that mediates precipitation of porous silica within minutes after the addition of silicic acid. Remarkably, the precipitate displays pore sizes in the range 100–1000 nm, which is characteristic for diatom biosilica nanopatterns (see reference 19).
[114] Chang J-S, Kong Z-L, Hwang D-F, Chang KLB. Chem Mater 2006;18:702–7.
[115] Patwardhan SV, Belton DJ, Shirtcliffe NJ. Chem Mater 2006;18:1711–2.
[116] This is reminiscent of the term "threshold inhibition" which is a widespread approach to interpret inhibition of sparingly soluble inorganic salts (such as calcium carbonate(s), phosphate(s) and sulfate(s), etc.) by organic additives (such as phosphonates, carboxylates and anionic polymers). Inhibition in this situation is achieved by additives added in sub-stoichiometric amounts. For some representative examples see references 117–120.
[117] Barouda E, Demadis KD, Freeman S, Jones F, Ogden MI. Cryst Growth Des 2007;7:321–7.
[118] Meldrum FC. Int Mater Rev 2003;48:187–224.
[119] de Leeuw NH, Cooper TG. Cryst Growth Des 2004;4:123–33.
[120] Lin Y-P, Singer PC. Water Res 2005;39:4835–43.
[121] Knecht MR, Wright DW. Langmuir 2004;20:4728–32.
[122] Patwardhan SV, Maheshwari R, Mukherjee N, Kiick KL, Clarson SJ. Biomacromolecules 2006;7:491–7.
[123] Abendroth RP. J Colloid Interface Sci 1970;34:591–6.
[124] Bolt GH. J Phys Chem 1957;61:1166–9.
[125] Sposito GJ. J Colloid Interface Sci 1983;91:329–40.
[126] Schindler P, Kamber HR. Helv Chim Acta 1968;51:1781–6.
[127] Zhuravlev LT. Colloids Surf A 1993;74:71–90.
[128] Abendroth RP. J Phys Chem 1972;76:2547–9.
[129] Zhuravlev LT. Colloids Surf A 2000;173:1–38.
[130] Iler RK. J Chromatogr 1981;209:341–2.
[131] Tilburey GE, Patwardhan SV, Huang J, Kaplan DL, Perry CC. J Phys Chem B 2007;111:4630–8.
[132] Belton D, Paine G, Patwardhan SV, Perry CC. J Mater Chem 2004;14:2231–41.
[133] Rodriguez F, Glawe DD, Naik RR, Hallinan KP, Stone MO. Biomacromolecules 2004;5:261–5.
[134] Tomczak MM, Glawe DD, Drummy LF, Lawrence CG, Stone MO, Perry CC, et al. J Am Chem Soc 2005;127:12577–82.
[135] Coffman EA, Melechko AV, Allison DP, Simpson ML, Doktycz MJ. Langmuir 2004;20:8431–6.
[136] Jia Y, Gray GM, Hay JN, Li Y, Unali GF, Baines FL, et al. J Mater Chem 2005;15: 2202–9.
[137] Jia P-X, Fukazawa N, Jin R-H. Small 2007;3:394–8.
[138] Yuan JJ, Jin RH. Adv Mater 2005;17:885–8.
[139] Hukkamaki J, Pakkanen TT. Microporous Mesoporous Mater 2003;65:189–96.
[140] Shan W, Wang B, Zhang Y, Tang Y. Chem Commun 2005:1877–9.
[141] Kim DJ, Lee K-B, Lee TG, Shon HK, Kim W-J, Paik H-J, et al. Small 2005;1:992–6.
[142] Demadis KD, Mavredaki E, Stathoulopoulou A, Neofotistou A, Mantzaridis C. Desalination 2007;213:38–46.
[143] Annenkov VV, Danilovtseva EN, Likhoshway YV, Patwardhan SV, Perry CC. J Mater Chem 2008;18:553–9.
[144] Annenkov VV, Danilovtseva EN, Aseyev VO, Patwardhan SV, Perry CC. Proceedings of the IASTED International Conference Nanotechnology and Applications (NANA2008); 2008. p. 47–52.
[145] We have also used long, short and medium length diphosphonium-based polymers with ethylene oxide (EO) linking the phosphonium groups and studied their effect on silica formation. Soluble silicic acid levels of up to 270 ppm were achieved, higher than the control, at 40 ppm additive level. This work is in progress and will be published in the near future.
[146] Wetherbee R. Science 2002;298:547.
[147] Kinrade SD, Gillson A-ME, Knight CTG. Dalton Trans 2002:307–9.
[148] Kinrade SD, Hamilton RJ, Schach AS, Knight CTG. J Chem Soc Dalton Trans 2001:961–3.
[149] Kinrade SD, Schach AS, Hamilton RJ, Knight CTG. Chem Comm 2001:1564–5.
[150] Perry CC, Keeling-Tucker T. Chem Comm 1998:2587–8.
[151] Wenzl S, Hett R, Richthammer P, Sumper M. Angew Chem Int Ed 2008;47: 1729–32.
[152] Thamatrakoln K, Alverson AJ, Hildebrand M. J Phycol 2006;42:822–34.
[153] Thamatrakoln K, Hildebrand M. J Nanosci Nanotechnol 2005;5:158–66.
[154] Hildebrand M. J Nanosci Nanotechnol 2005;5:146–57.
[155] Stöber W, Fink A, Bohn E. J Colloid Interface Sci 1968;26:62–8.
[156] Fotou GP, Pratsinis SE, Pinto NG. J Non-Cryst Solids 1995;183:135–43.
[157] Benmouhoub N, Simmonet N, Agoudjil N, Coradin T. Green Chem 2008;10:957–64.
[158] Yang Y, Coradin T. Green Chem 2008;10:183–90.